0090-9556/07/3504-583–589$20.00
DRUG METABOLISM AND DISPOSITION

DMD 35:583–589, 2007

Vol. 35, No. 4
13706/3189591
Printed in U.S.A.

Glucuronidation of Antiallergic Drug, Tranilast: Identification of Human UDP-Glucuronosyltransferase Isoforms and Effect of Its Phase I Metabolite

Miki Katoh, Tomohito Matsui, and Tsuyoshi Yokoi

Division of Pharmaceutical Sciences, Graduate School of Medical Science, Kanazawa University, Kanazawa, Japan

Received November 5, 2006; accepted January 10, 2007

ABSTRACT:

Tranilast is an oral antiallergic agent widely used in Japan. Recently, in Western populations, hyperbilirubinemia induced by tranilast was suspected during clinical trials. Tranilast has been reported to be mainly metabolized to a glucuronide and a phase I metabolite, 4-demethyltranilast (N-3). In the present study, we investigated the in vitro metabolism of tranilast in human liver and jejunum microsomes and recombinant UDP-glucuronosyltransferases (UGTs). The glucuronidation of tranilast was clarified to be mainly catalyzed by UGT1A1 in human liver and intestine. The K_m values of tranilast glucuronosyltransferase activity were 51.5, 50.6, and 38.0 μM in human liver microsomes, human jejunum microsomes, and recombinant UGT1A1, respectively. The V_{max} values were 10.4, 42.9, and 19.7 pmol/min/mg protein in human liver microsomes, human jejunum microsomes, and recombinant UGT1A1, respectively. When the intrinsic clearance was calculated using the in vitro kinetic parameters, microsomal protein content, and weight of tissues, tranilast glucuronosyltransferase activity was 2.5-fold higher in liver than in intestine. Tranilast glucuronosyltransferase activity was strongly inhibited by bilirubin, a typical UGT1A1 substrate, and N-3, indicating that the phase I metabolite could affect the tranilast glucuronosyltransferase activity. In the case of N-3 formation, the K_m and V_{max} values were 37.1 μM and 27.6 pmol/min/mg protein in human liver microsomes. The bilirubin glucuronosyltransferase activity was strongly inhibited by both tranilast and N-3, suggesting that tranilast-induced hyperbilirubinemia would be responsible for the inhibition by tranilast and N-3 of the bilirubin glucuronosyltransferase activity, as would the *UGT1A1* genotype.

Tranilast (*N*-(3′,4′-demethoxycinnamoyl)-anthranilic acid) is an oral antiallergic agent developed by Kissei Pharmaceutical Co. Ltd. (Nagano, Japan) and widely used in Japan for bronchial asthma, allergic rhinitis, atopic dermatitis, keloid, and hypertrophic scar. The mechanism of its efficacy is to inhibit chemical mediators from mast cells (Azuma et al., 1976) and the accumulation of collagen in granulation tissue (Isaji et al., 1987). Recently, a clinical trial regarding the prevention of restenosis after percutaneous transluminal coronary revascularization was performed in Western populations (Holmes et al., 2000). During that trial, it was found that hyperbilirubinemia might be induced by tranilast and the risk of hyperbilirubinemia was increased in individuals with Gilbert's syndrome (Danoff et al., 2004).

Major metabolic pathways of tranilast have been shown to be glucuronidation, 4-demethylation (N-3), and sulfation of N-3 in the data sheet of tranilast provided by Kissei Pharmaceutical (Fig. 1). Tranilast, N-3, and N-3 sulfate were reported to be detected in human urine (Slobodzian et al., 1985). Since the urine sample was hydrolyzed by glucuronidase and/or base in that article, the formation of glucuronide could be speculated by a comparison of the chromatograms before and after hydrolysis. The major metabolites of tranilast in urine in human were tranilast glucuronide and N-3 sulfate and their recoveries were almost the same (unpublished report from Kissei Pharmaceutical). Although phase I metabolism of tranilast was shown to be mainly catalyzed by CYP2C9 in humans (unpublished data from Kissei Pharmaceutical), tranilast metabolism in glucuronidation still remains uncertain.

In the case of many drugs, since a parent drug and/or its phase I metabolite could be conjugated with glucuronic acid, the role of UDP-glucuronosyltransferase (UGT) has recently received attention. The major metabolic pathway of a drug is not always catalyzed by cytochrome P450. In the case of tranilast, N-3 formation was catalyzed by CYP2C9, and the possibility of drug interaction with warfarin was described in the data sheet of tranilast. However, the kinetics of tranilast glucuronidation is unknown. The purpose of the present study was to clarify the tranilast metabolism involving glucuronidation. In addition, to investigate the mechanism of tranilast-induced hyperbilirubinemia, the inhibitory effects of tranilast and N-3 on bilirubin glucuronosyltransferase activity were demonstrated.

Materials and Methods

Materials. Tranilast, 4-demethyltranilast, and 3-demethyltranilast (N-4) were kindly supplied by Kissei Pharmaceutical. UDP-glucuronic acid (UDP-GA), alamethicin, β-estradiol, emodin, and β-glucuronidase from *Helix pomatia* (type H-2) were purchased from Sigma-Aldrich (St. Louis, MO). Bilirubin, 4-nitrophenol, and imipramine hydrochloride were obtained from Wako

Article, publication date, and citation information can be found at http://dmd.aspetjournals.org.
doi:10.1124/dmd.106.013706.

ABBREVIATIONS: N-3, 4-demethyltranilast; UGT, UDP-glucuronosyltransferase; N-4, 3-demethytranilast; UDP-GA, UDP-glucuronic acid; HPLC, high-performance liquid chromatography; IS, internal standard; CL_{int}, intrinsic clearance.

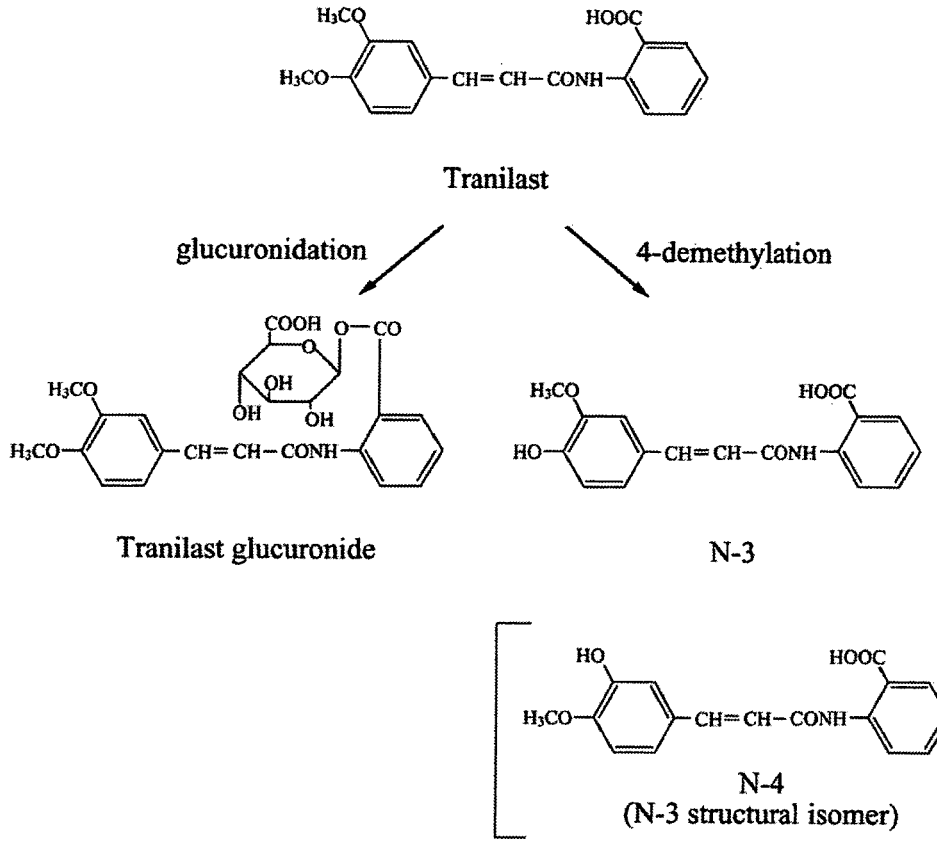

FIG. 1. Metabolic pathways of tranilast in humans.

Pure Chemicals (Osaka, Japan). Propofol was kindly provided by AstraZeneca (London, UK). Nicotinamide adenine dinucleotide phosphate (oxidized form, $NADP^+$) and glucose-6-phosphate dehydrogenase were purchased from Oriental Yeast (Tokyo, Japan). 7-Hydroxycoumarin was obtained from Invitrogen (Carlsbad, CA). Pooled human liver microsomes and microsomes from 22 individual human livers were purchased from BD Gentest (Woburn, MA). The glucuronosyltransferase activity of β-estradiol in these human individual liver microsomes was provided as the typical activity for UGT1A1 by the manufacturer. The human jejunum microsomes (HJM0040) were purchased from KAC (Kyoto, Japan). Recombinant human UGT1A8, UGT1A3, UGT1A4, UGT1A6, UGT1A7, UGT1A8, UGT1A9, UGT1A10, UGT2B4, UGT2B7, UGT2B15, and UGT2B17 expressed in baculovirus-infected insect cells were also obtained from BD Gentest. All other chemicals and solvents were of analytical or the highest grade commercially available.

Tranilast Glucuronidation Assay. A typical incubation mixture (total volume, 0.2 ml) contained 50 mM Tris-HCl buffer (pH7.4), 5 mM $MgCl_2$, 50 μg of alamethicin/mg microsomal protein, 5 mM UDP-GA, 0.5 mg/ml human liver microsomes, and tranilast. The reaction was initiated by the addition of UDP-GA and the mixture was then incubated for 60 min at 37°C. The reaction was terminated by boiling for 5 min. After removal of the protein by centrifugation at 9000*g* for 5 min, an 80-μl portion of the sample was subjected to high-performance liquid chromatography (HPLC) with a NovaPack Phenyl 4-μm analytical column (3.9 × 150 mm; Waters, Milford, MA). The product formation was measured as described previously (Slobodzian et al., 1985) with slight modifications. The mobile phase was methanol/50 mM sodium dihydrogen phosphate (pH 5.3), 40:60 (v/v) and the flow rate was 1.0 ml/min. The eluent was monitored at 335 nm with a noise-base clean Uni-3 (Union, Gunma, Japan). The retention times of tranilast glucuronide, tranilast, and 7-hydroxycoumarin (internal standard, IS) were 4.4, 10.0, and 3.6 min, respectively (Fig. 2). None of these chromatograms showed any interfering peaks with tranilast glucuronide. For the quantification of tranilast glucuronide, the eluate of the HPLC from the incubation mixture with human liver microsomes, including tranilast glucuronide, was collected with reference to the retention time. A part of the eluate was incubated with 1000 U/ml β-glucuronidase at 37°C for 24 h.

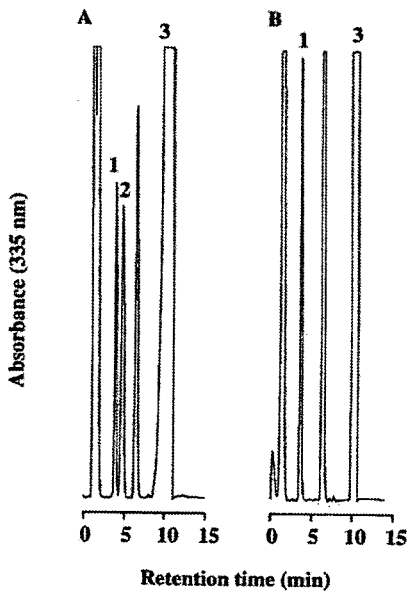

FIG. 2. Representative HPLC chromatograms of tranilast glucuronide in human liver microsomes. Tranilast was incubated at 37°C for 60 min with (A) or without (B) UDP-GA. Peak 1, 7-hydroxycoumarin (IS); peak 2, tranilast glucuronide; peak 3, tranilast.

The hydrolyzed tranilast glucuronide was quantified as tranilast by HPLC. Once we determined the peak area per known content of tranilast glucuronide, the ratio was applied to the calculation of the tranilast glucuronide formed in the incubation mixtures.

Kinetic Analyses. The kinetic studies were performed using human liver microsomes, human jejunum microsomes, and recombinant human UGT1A1

expressed in baculovirus-infected insect cells. When determining the kinetic parameters, the tranilast concentration ranged from 5 μM to 2 mM. The kinetic parameters were estimated from the fitted curves using a computer program, KaleidaGraph (Synergy Software, Reading, PA), designed for nonlinear regression analysis.

Correlation Analyses. The correlations between the tranilast glucuronosyltransferase activity and the other glucuronosyltransferase activities were determined by Pearson's product moment method. A p value of less than 0.05 was considered statistically significant.

Inhibition Analysis of Tranilast Glucuronosyltransferase Activity in Human Liver and Jejunum Microsomes. As described by Watanabe et al. (2002), bilirubin (UGT1A1), β-estradiol (UGT1A1 and UGT1A9), 4-nitrophenol (UGT1A6 and UGT1A9), imipramine (UGT1A3 and UGT1A4), emodin (UGT1A8 and UGT1A10), and propofol (UGT1A9) are typical substrates for each UGT isoform. These six substrates were investigated for their inhibitory effects on the tranilast glucuronosyltransferase activity. For the determination of the IC_{50} values, the concentration of tranilast was set at 100 μM. The final concentration of the organic solvents in the reaction mixture was <2% (v/v). The tranilast glucuronosyltransferase activities in pooled human liver microsomes and human jejunum microsomes (HJM0040) at 100 μM tranilast were determined as described above.

Inhibition of N-3 and N-4 on Tranilast Glucuronosyltransferase Activity in Human Liver and Jejunum Microsomes. The inhibition of N-3, a phase I metabolite of tranilast, and N-4, a structural isomer of N-3, on the tranilast glucuronosyltransferase activity was also investigated in pooled human liver microsomes and individual human jejunum microsomes. For the determination of the IC_{50} values, the concentration of tranilast was set at 100 μM. For the determination of the K_i values in pooled human liver microsomes, the concentrations of tranilast, N-3, and N-4 ranged from 10 to 160 μM, 0 to 150 μM, and 0 to 30 μM, respectively. The K_i values were estimated from the fitted curve using a computer program (K cat; BioMetallics, Princeton, NJ) designed for nonlinear regression analysis.

Tranilast 4-Demethylation Assay. A typical incubation mixture (total volume, 0.2 ml) contained 100 mM Tris-HCl buffer (pH7.4), 0.2 mg/ml human liver microsomes, an NADPH-generating system (0.5 mM $NADP^+$, 5 mM glucose 6-phosphate, 5 mM $MgCl_2$, and 1 U/ml glucose-6-phosphate dehydrogenase), and tranilast. The reaction was initiated by the addition of the NADPH-generating system and was then incubated for 30 min at 37°C. The reaction was terminated by adding 100 μl of ice-cold methanol. 7-Hydroxycoumarin was added as an IS. After removal of the protein by centrifugation at 9000g for 5 min, an 80-μl portion of the sample was subjected to HPLC. The product formation was measured using the same method for tranilast glucuronide except the mobile phase. The mobile phase was methanol/50 mM sodium dihydrogen phosphate (pH 5.3), 33:67 (v/v). The retention times of N-3, tranilast, and 7-hydroxycoumarin (IS) were 9.8, 21.4, and 4.7 min, respectively. None of these chromatograms showed any interfering peaks with N-4 (data not shown).

The kinetic studies were performed using human liver microsomes. In determining the kinetic parameters, the tranilast concentration ranged from 2 to 500 μM. Kinetic parameters were estimated from the fitted curves using the computer program KaleidaGraph (Synergy Software) designed for nonlinear regression analysis.

Inhibition of Tranilast, N-3, and N-4 on Bilirubin Glucuronosyltransferase Activity in Human Live Microsomes. A typical incubation mixture (total volume, 0.2 ml) contained 50 mM Tris-HCl buffer (pH 7.4), 5 mM $MgCl_2$, 50 μg of alamethicin/mg microsomal protein, 2 mM UDP-GA, 0.5 mg/ml human liver microsomes, 10 μM bilirubin, and tranilast (N-3 or N-4). The reaction was initiated by the addition of UDP-GA and was then incubated for 30 min at 37°C. The reaction was terminated by adding 100 μl of ice-cold methanol. After removal of the protein by centrifugation at 9000g for 5 min, a 50-μl portion of the sample was subjected to HPLC with a Develosil C_{30} 5-μm analytical column (4.6 × 150 mm; Nomura Chemical, Aichi, Japan). The product formation was measured as described previously (Luquita et al., 2001) with slight modifications. The mobile phase was 55% methanol/50 mM potassium dihydrogen phosphate and the flow rate was 1.0 ml/min. The eluent was monitored at 450 nm with a noise-base clean Uni-3 (Union). The final concentration of the organic solvents in the reaction mixture was <2% (v/v).

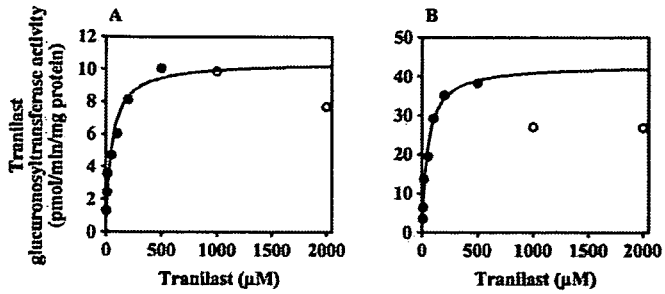

FIG. 3. Kinetic analyses of tranilast glucuronosyltransferase activity in human liver (A) or jejunum (B) microsomes. The solid line represents the curve fitting the Michaelis-Menten equation (5 to 500 μM, closed circles). The tranilast glucuronosyltransferase activity was determined as described under *Materials and Methods*. Each data point represents the mean of duplicate determinations.

Results

Kinetics of Tranilast Glucuronosyltransferase Activity in Human Liver or Jejunum Microsomes. Kinetic analyses of tranilast glucuronidation in human liver or jejunum microsomes were performed. As shown in Fig. 3, A and B, the kinetics of 5 to 500 μM tranilast fitted to the Michaelis-Menten kinetics in both human liver and jejunum microsomes. However, when the tranilast concentration exceeded 500 μM in human liver microsomes, the tranilast glucuronosyltransferase activity gradually decreased. In human jejunum microsomes, the tranilast glucuronosyltransferase activity was also decreased at 1 and 2 mM compared with 500 μM. When the apparent kinetic parameters were estimated by fitting to the Michaelis-Menten equation with the initial velocity values at 5 to 500 μM tranilast, the K_m values in human liver and jejunum microsomes were 51.5 ± 12.8 and 50.6 ± 5.7 μM, respectively, and the V_{max} values were 10.4 ± 0.8 and 42.9 ± 1.5 pmol/min/mg protein, respectively.

Tranilast Glucuronosyltransferase Activity in Recombinant UGT Isoforms. The recombinant UGT isoforms expressed in baculovirus-infected insect cells were used to determine their tranilast glucuronosyltransferase activities (Fig. 4A). UGT1A1 exhibited the highest tranilast glucuronosyltransferase activity (13.5 pmol/min/mg protein). UGT1A3, UGT1A8, UGT1A9, and UGT1A10 exhibited low tranilast glucuronosyltransferase activities.

Kinetics of Tranilast Glucuronosyltransferase Activity in Recombinant UGT1A1. As shown in Fig. 4B, the kinetics of tranilast glucuronidation in recombinant UGT1A1 at 5 to 500 μM tranilast fitted to the Michaelis-Menten kinetics. However, when the tranilast concentration exceeded 500 μM, the tranilast glucuronosyltransferase activity gradually decreased as in the case of human liver and jejunum microsomes. When the apparent kinetic parameters were estimated with the initial velocity values at 5 to 500 μM tranilast, the K_m value was 38.0 ± 5.6 μM and the V_{max} value was 19.7 ± 0.8 pmol/min/mg protein.

Interindividual Variability of Tranilast Glucuronosyltransferase Activity from 22 Human Livers and Correlation Analyses. The tranilast glucuronosyltransferase activities in microsomes from 22 human livers were determined at 40 μM tranilast (Fig. 5, top). The tranilast glucuronosyltransferase activity ranged from 1.9 pmol/min/mg protein in HG93 to 18.3 pmol/min/mg protein in HH31. The interindividual variability in the tranilast glucuronosyltransferase activity was 9.5-fold. Correlation analyses were performed between the tranilast glucuronosyltransferase activity and bilirubin (UGT1A1), β-estradiol (UGT1A1), etoposide (UGT1A1), trifluoperazine (UGT1A4), propofol (UGT1A9), or morphine glucuronosyltransferase activities (UGT2B7) provided by the manufacturer (Table 1).

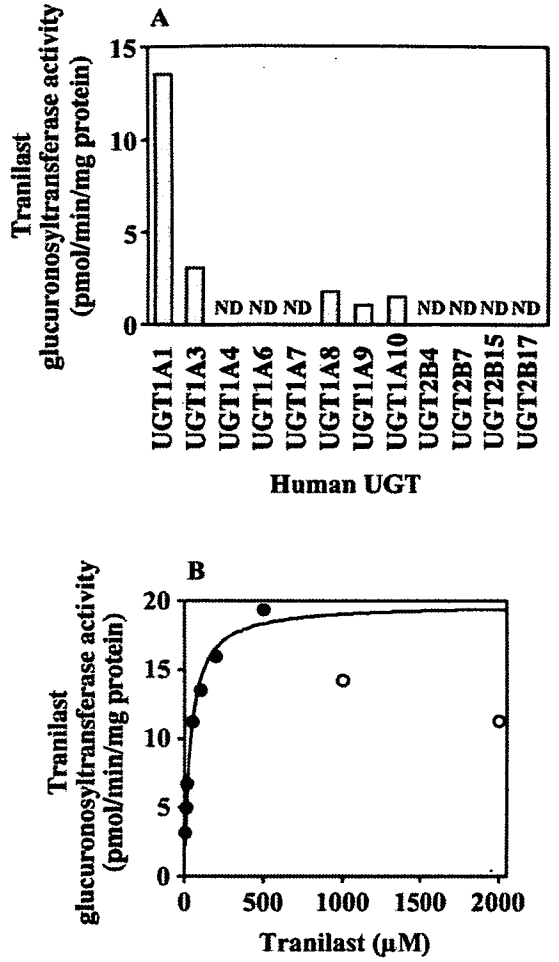

FIG. 4. Tranilast glucuronosyltransferase activity in recombinant human UGTs in baculovirus-infected insect cells (A) and kinetic analysis in UGT1A1 (B). A, the concentration of tranilast was 100 μM. Each column represents the mean of duplicate determinations. ND, not detected. B, the solid line represents the curve fitting the Michaelis-Menten equation (5–500 μM, closed circles). Each data point represents the mean of duplicate determinations.

The etoposide glucuronosyltransferase activities (UGT1A1) were measured in our laboratory according to the method of Watanabe et al. (2002). Since we could not obtain those activities in all individual liver microsomes, correlation analyses among bilirubin, etoposide, and morphine glucuronosyltransferase activities were performed using 11 of 22 liver microsomes. The tranilast glucuronosyltransferase activities in individual human liver microsomes were significantly correlated with the β-estradiol ($r = 0.956, p < 0.0001$), bilirubin ($r = 0.937, p < 0.0001$), and propofol ($r = 0.449, p < 0.05$) glucuronosyltransferase activities. The tranilast glucuronosyltransferase activities did not correlate with the trifluoperazine ($r = 0.179$) and morphine ($r = 0.257$) glucuronosyltransferase activities.

Inhibition Analyses of Glucuronosyltransferase Activity in Human Liver or Jejunum Microsomes. The inhibitory effects of bilirubin, β-estradiol, 4-nitrophenol, imipramine, emodin, and propofol on the tranilast glucuronosyltransferase activity in human liver and jejunum microsomes were determined. As shown in Fig. 6A, the tranilast glucuronosyltransferase activity in pooled human liver microsomes was inhibited by bilirubin ($IC_{50} = 123.9$ μM). As shown in Fig. 6B, the activity in human jejunum microsomes was strongly inhibited by bilirubin ($IC_{50} = 81.1$ μM) and β-estradiol ($IC_{50} = 75.3$ μM).

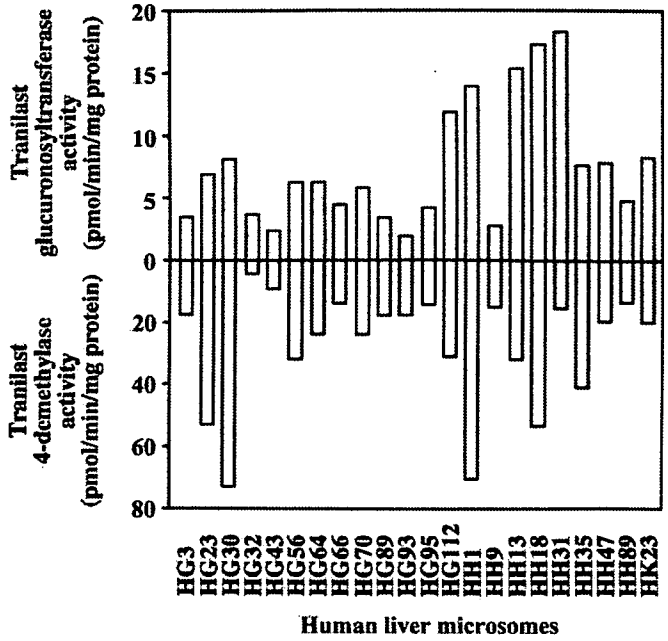

FIG. 5. Interindividual variability of tranilast glucuronosyltransferase activity (A) and 4-demethylase activity (B) in microsomes from 22 human livers. In A and B, the concentration of tranilast was 40 μM. Each column represents the mean of duplicate determinations.

Inhibition of N-3 and N-4 on Tranilast Glucuronosyltransferase Activity in Human Liver and Jejunum Microsomes. The inhibitory effects of N-3 and N-4 on the tranilast glucuronosyltransferase activity in human liver and jejunum microsomes were determined. The tranilast glucuronosyltransferase activities in human liver and jejunum microsomes were strongly inhibited by both N-3 and N-4 (Fig. 6). The IC_{50} values of N-3 and N-4 were 141.7 and 81.3 μM, respectively, in liver microsomes and 82.8 and 45.9 μM, respectively, in jejunum microsomes. The inhibition pattern of N-3 was competitive. The K_{is} value of N-3 for the tranilast glucuronosyltransferase activity in human liver microsomes was 52.8 μM (Fig. 7). On the other hand, the inhibition pattern of N-4 was mixed. The K_{is} and K_{ii} values of N-4 for the tranilast glucuronosyltransferase activity in human liver microsomes were 42.6 and 181.1 μM, respectively (Fig. 7).

Kinetics of Tranilast 4-Demethylase Activity in Human Liver Microsomes. The kinetics of tranilast 4-demethylation (N-3 formation) in pooled human liver microsomes at 2 to 500 μM tranilast fitted to the Michaelis-Menten kinetics. The K_m and V_{max} values were 37.1 ± 3.1 μM and 27.6 ± 0.7 pmol/min/mg protein, respectively.

Interindividual Variability of Tranilast 4-Demethylase Activity from 22 Human Livers and Correlation Analyses. The tranilast 4-demethylase activities in microsomes from 22 human livers were determined at 40 μM tranilast. The interindividual variability in the tranilast glucuronosyltransferase activity was at most 16.4-fold (Fig. 5, bottom). The tranilast 4-demethylase activity ranged from 4.5 pmol/min/mg protein in HG32 to 73.1 pmol/min/mg protein in HG30. Correlation analyses were performed between the tranilast 4-demethylase activity and phenacetin *O*-deethylase activity (CYP1A2), coumarin 7-hydroxylase activity (CYP2A6), *S*-mephenytoin *N*-demethylase activity (CYP2B6), paclitaxel 6α-hydroxylase activity (CYP2C8), diclofenac 4′-hydroxylase activity (CYP2C9), *S*-mephenytoin 4′-hydroxylase activity (CYP2C19), bufuralol 1′-hydroxylase activity (CYP2D6), chlorzoxazone 6-hydroxylase activity (CYP2E1), testosterone 6β-hydroxylase activity (CYP3A4), or lauric acid 12-

TABLE 1

Correlation between tranilast glucuronosyltransferase activity and other glucuronosyltransferase activities in individual human liver microsomes

Glucuronidation	*n*	Substrate	*r*	*p*
		μM		
Bilirubin glucuronidation	11	10	0.963	<0.0001
β-Estradiol 3-glucuronidation	22	100	0.965	<0.0001
Etoposide glucuronidation	11	400	0.829	<0.01
Trifluoperazine glucuronidation	22	100	0.179	N.S.
Propofol glucuronidation	22	30	0.449	<0.05
Morphine 3-glucuronidation	11	250	0.257	N.S.

n, number of individual human liver microsomes; N.S., not significant.

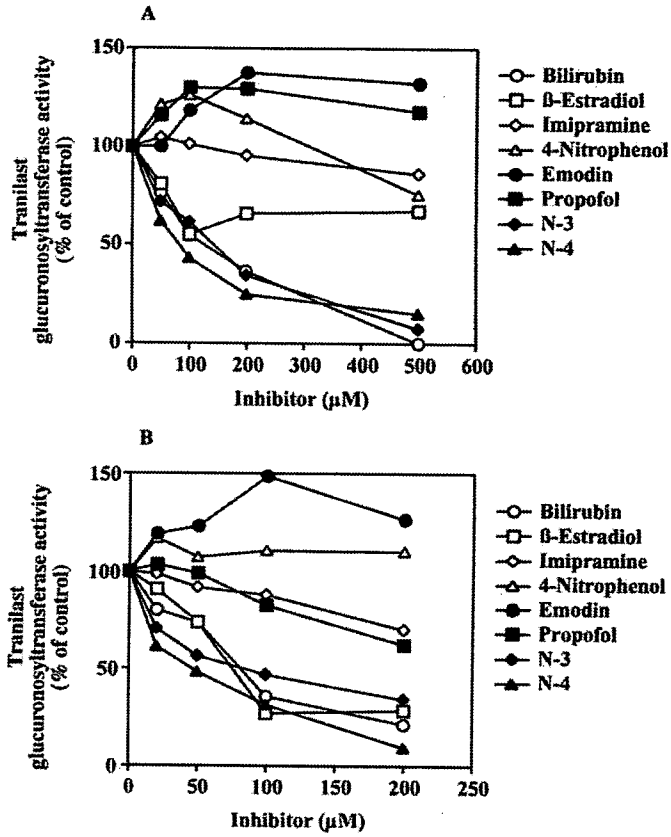

FIG. 6. Inhibitory effects of typical substrates for UGT isoforms, N-3, and N-4 on tranilast glucuronosyltransferase activity in human liver (A) or jejunum (B) microsomes. Bilirubin (UGT1A1), β-estradiol (UGT1A1 and UGT1A9), imipramine (UGT1A3 and UGT1A49), 4-nitrophenol (UGT1A6 and UGT1A9), emodin (UGT1A8 and UGT1A10), propofol (UGT1A9), N-3, and N-4 were used as inhibitors. Each data point represents the mean of duplicate determinations. The control activity was 6.2 pmol/min/mg protein in human liver microsomes and 24.0 pmol/min/mg protein in human jejunum microsomes, respectively.

hydroxylase activity (CYP4A) provided by the manufacturer. The tranilast 4-demethylase activities in the 22 human liver microsomes were significantly correlated with the diclofenac 4′-hydroxylase activities ($r = 0.825$, $p < 0.0001$) and the paclitaxel 6α-hydroxylase activities ($r = 0.576$, $p < 0.01$).

Inhibition of Tranilast, N-3, and N-4 on Bilirubin Glucuronosyltransferase Activity in Human Liver Microsomes. The inhibitory effects of tranilast, N-3, and N-4 on the bilirubin glucuronosyltransferase activity in human liver microsomes were determined. The bilirubin glucuronosyltransferase activity was strongly inhibited by tranilast, N-3, and N-4. The IC_{50} values of tranilast, N-3, and N-4 were 28.7, 76.9, and 62.0 μM, respectively.

Discussion

Although tranilast has been prescribed for many decades in Japan, its metabolism has not been investigated completely. In human, the major metabolites have been reported to be tranilast glucuronide and N-3 sulfate (unpublished data, Kissei Pharmaceutical). In human urine, other metabolites such as N-2 [2-(4′-hydroxy-3′-methoxystyryl)-3,1-benzoxazin-4-one], N-6 (1-benzoxazin-4-one), and N-3 glucuronide (unpublished data, Kissei Pharmaceutical) were slightly detected. In the present study, it was clarified that tranilast glucuronidation was mainly catalyzed by UGT1A1 in human. UGT1A3, UGT1A8, and UGT1A10 were partly responsible for the tranilast glucuronidation. The tranilast glucuronosyltransferase activity could be detected in both human liver and jejunum microsomes. UGT1A1 is one of the major isoforms of UGTs in the liver and is also expressed in the intestine. UGT1A8 and UGT1A10 could be responsible for the extrahepatic metabolism of tranilast because these isoforms are expressed in the intestine but not in liver. However, the tranilast glucuronosyltransferase activity in human jejunum microsomes was inhibited by bilirubin and β-estradiol but not by emodin (Fig. 6B), suggesting that the tranilast glucuronosyltransferase activity was mainly catalyzed by UGT1A1 in intestine as in the liver.

The tranilast glucuronosyltransferase activity was reduced at high substrate concentrations (>500 μM) in human liver and jejunum microsomes and recombinant UGT1A1. The reason for this phenomenon was unclear, but substrate and/or metabolite inhibition may be involved. Further study is needed to clarify the mechanism of the inhibition. The maximum serum concentration of tranilast in humans has been reported to be 37.0 μM after single oral administration at the therapeutic dose of 100 mg (Slobodzian et al., 1985). As reported by Kissei Pharmaceutical, the maximum serum concentration of tranilast was 67.8 μM after taking 2.5 mg/kg tranilast three times per day for 5 days. In clinical practice, the concentration of tranilast is unlikely to reach 500 μM. Therefore, the kinetic parameters fitted to the Michaelis-Menten equation with <500 μM tranilast seems to be reasonable.

The in vitro intrinsic clearance (CL_{int}) is calculated using the following equation (Obach et al., 1997; Soars et al., 2002): $CL_{int} = [V_{max}/K_m] \times$ [microsomal protein/tissue (mg/g)] × [tissue/body weight (g/kg)]. Soars et al. (2002) reported that there were 45 mg of microsomal protein/g of liver and 20 g of liver/kg of body weight. The CL_{int} in liver of tranilast was calculated to be 181.7 μl/min/kg. They also reported that there are 3 mg of microsomal protein/g of intestine and 30 g of intestine/kg of body weight (Soars et al., 2002). The CL_{int} in intestine was estimated to be 76.3 μl/min/kg. The glucuronosyltransferase activity has been reported to differ according to regions of the intestine in humans (Strassburg et al., 2000). The UGT1A1 activity in humans was higher in upper intestine than lower intestine (Basu et al., 2004). Although the UGT activity in the intestine may differ from that in the liver, the tranilast glucuronosyltransferase activity in the intestine might be approximately 40% of that in the liver.

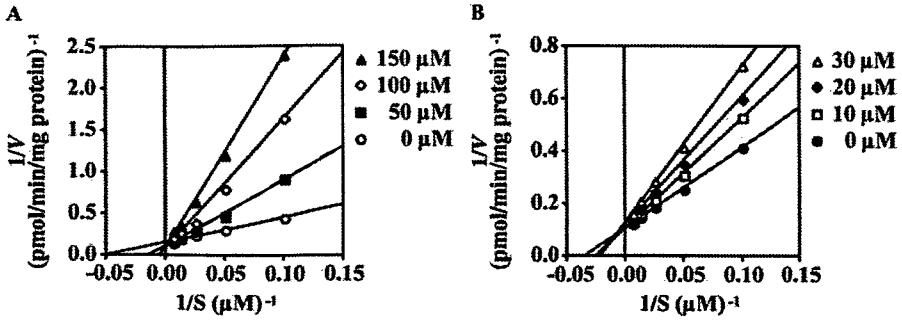

FIG. 7. Inhibitory effect of N-3 (A) and N-4 (B) on tranilast glucuronosyltransferase activity in human liver microsomes. Human liver microsomes were incubated with tranilast in the absence or presence of N-3 and N-4 as described under *Materials and Methods*. Each data point represents the mean of duplicate determinations.

UGT1A1 has shown polymorphic metabolism. Particularly, the relationship between the toxicity of irinotecan hydrochloride and the *UGT1A1* genotype has been extensively studied (Ando et al., 2005). As well as irinotecan hydrochloride, *UGT1A1* genetic polymorphism would affect the tranilast pharmacokinetics.

Another metabolic pathway of tranilast is N-3 formation catalyzed by CYP2C9 (unpublished data, Kissei Pharmaceutical). We first analyzed the kinetics of tranilast 4-demethylase activity in human liver microsomes. The K_m value of N-3 formation in human liver microsomes was 37.1 ± 3.1 μM, which was similar to that of the tranilast glucuronosyltransferase activity. There was large interindividual variability (>16-fold) in the N-3 formation. In CYP2C9, several polymorphic alleles have been reported to have decreased enzyme activity in vitro and in vivo (Takahashi et al., 1998; Blaisdell et al., 2004). The frequency of poor metabolizing alleles such as *CYP2C9*2* and *CYP2C9*3* was different between ethnic groups (Sullivan-Klose et al., 1996; Blaisdell et al., 2004). Therefore, the genetic polymorphisms of *CYP2C9* and *UGT1A1* would play important roles in the pharmacokinetics of tranilast.

In the present study, N-3 was demonstrated to inhibit tranilast glucuronosyltransferase activity. Although the concentration of N-3 in the liver is unknown, N-3 could affect tranilast glucuronosyltransferase activity, leading to altered pharmacokinetics of tranilast. N-3 is further metabolized to be N-3 glucuronide and could be slightly detected in human urine (unpublished data, Kissei Pharmaceutical). Since the inhibition pattern of N-3 on tranilast glucuronosyltransferase activity was competitive, the glucuronidation of N-3 might be catalyzed by UGT1A1. N-4, a structural isomer of N-3, also inhibited tranilast glucuronosyltransferase activity. However, there are no reports that N-4 could be detected in humans. Because glucuronidation of a drug may be inhibited by its cytochrome P450 metabolites, the inhibition by metabolites should be kept in mind when estimating the pharmacokinetics.

Recently, the PRESTO (prevention of restenosis with tranilast and its outcomes) study was performed in Western populations because tranilast may have a benefit in preventing restenosis after percutaneous transluminal coronary revascularization (Holmes et al., 2000). During the phase III clinical trial, an increase in serum unconjugated bilirubin was observed in 12% of white subjects (Danoff et al., 2004). It was suspected that tranilast-induced hyperbilirubinemia might be caused by the inhibition by tranilast and N-3 of bilirubin glucuronosyltransferase activity. Danoff et al. (2004) suggested that tranilast-induced hyperbilirubinemia might be related to genetic polymorphisms of *UGT1A1*. As reported by Kissei Pharmaceutical, the frequencies of liver dysfunction and jaundice caused by tranilast were 0.62 and 0.008%, respectively, in Japanese. The frequency of hyperbilirubinemia in Japanese is unknown but seems to be lower than that in white subjects. The reason for this phenomenon may be interethnic variability in the *UGT1A1* allelic frequency. In the case of *UGT1A1*28*, which is mainly responsible for Gilbert's syndrome, its allelic frequency has been shown to be 35.7 to 41.3% in whites (Monaghan et al., 1996, 1997) but 13.8% in Asians (Ando et al., 1998). In patients with Gilbert's syndrome, the unconjugated bilirubin concentration may be significantly elevated after tranilast administration because of the inhibition of UGT1A1 activity by tranilast and N-3. In addition, as mentioned above, the allele frequency of the *CYP2C9* poor metabolizer was higher in whites than in Japanese (Nasu et al., 1997; Scordo et al., 2001). Thus, the genetic risk for the elevation of tranilast concentration would be higher in whites than in Japanese. The occurrence of adverse reactions from tranilast might be explained by the enzyme inhibition and the genetic polymorphisms of both phase I and phase II enzymes.

In conclusion, it was clarified that the tranilast glucuronosyltransferase activity was mainly catalyzed by UGT1A1 in human liver and intestine. N-3, a phase I metabolite of tranilast, inhibited the tranilast glucuronosyltransferase activity, suggesting that the inhibition by a phase I metabolite may be noteworthy when estimating the glucuronidation of a drug. The inhibition by tranilast and N-3 of the bilirubin glucuronosyltransferase activity may be partly responsible for tranilast-induced hyperbilirubinemia. We should keep in mind that UGT1A1 substrates may inhibit the bilirubin glucuronosyltransferase activity leading to hyperbilirubinemia, and that phase I metabolites can affect the glucuronidation of its parent drug.

Acknowledgments. We acknowledge Kissei Pharmaceutical for kindly providing tranilast, N-3, and N-4, and Brent Bell for reviewing the manuscript.

References

Ando Y, Chida M, Nakayama K, Saka H, and Kamataki T (1998) The *UGT1A1*28* allele is relatively rare in a Japanese population. *Pharmacogenetics* **8**:357–360.

Ando M, Hasegawa Y, and Ando Y (2005) Pharmacogenetics of irinotecan: a promoter polymorphism of UGT1A1 gene and severe adverse reactions to irinotecan. *Investig New Drugs* **23**:539–545.

Azuma H, Banno K, and Yoshimura T (1976) Pharmacological properties of N-(3',4'-dimethoxycinnamoyl) anthranilic acid (N-5'), a new anti-atopic agent. *Br J Pharmacol* **58**:483–488.

Basu NK, Ciotti M, Hwang MS, Kole L, Mitra PS, Cho JW, and Owens IS (2004) Differential and special properties of the major human UGT1-encoded gastrointestinal UDP-glucuronosyltransferases enhance potential to control chemical uptake. *J Biol Chem* **279**: 1429–1441.

Blaisdell J, Jorge-Nebert LF, Coulter S, Ferguson SS, Lee SJ, Chanas B, Xi T, Mohrenweiser H, Ghanayem B, and Goldstein JA (2004) Discovery of new potentially defective alleles of human *CYP2C9*. *Pharmacogenetics* **14**:527–537.

Danoff TM, Campbell DA, McCarthy LC, Lewis KF, Repasch MH, Saunders AM, Spurr NK, Purvis IJ, Roses AD, and Xu CF (2004) A Gilbert's syndrome *UGT1A1* variant confers susceptibility to tranilast-induced hyperbilirubinemia. *Pharmacogenomics J* **4**:49–53.

Holmes D, Fitzgerald P, Goldberg S, LaBlanche J, Lincoff AM, Savage M, Serruys PW, Willerson J, Granett JR, Chan R, et al. (2000) The PRESTO (Prevention of restenosis with tranilast and its outcomes) protocol: a double-blind, placebo-controlled trial. *Am Heart J* **139**:23–31.

Isaji M, Nakajoh M, and Naito J (1987) Selective inhibition of collagen accumulation by N-(3,4-dimethoxycinnamoyl)anthranilic acid (N-5') in granulation tissue. *Biochem Pharmacol* **36**:469–474.

Luquita MG, Catania VA, Pozzi EJ, Veggi LM, Hoffman T, Pellegrino JM, Ikushiro Si, Emi Y, Iyanagi T, Vore M, et al. (2001) Molecular basis of perinatal changes in UDP-glucuronosyltransferase activity in maternal rat liver. *J Pharmacol Exp Ther* **298**:49–56.

Monaghan G, Foster B, Jurima-Romet M, Hume R, and Burchell B (1997) UGT1*1 genotyping in a Canadian Inuit population. *Pharmacogenetics* **7**:153–156.
Monaghan G, Ryan M, Seddon R, Hume R, and Burchell B (1996) Genetic variation in bilirubin UPD-glucuronosyltransferase gene promoter and Gilbert's syndrome. *Lancet* **347**:578–581.
Nasu K, Kubota T, and Ishizaki T (1997) Genetic analysis of *CYP2C9* polymorphism in a Japanese population. *Pharmacogenetics* **7**:405–409.
Obach RS, Baxter JG, Liston TE, Silber BM, Jones BC, MacIntyre F, Rance DJ, and Wastall P (1997) The prediction of human pharmacokinetic parameters from preclinical and in vitro metabolism data. *J Pharmacol Exp Ther* **283**:46–58.
Scordo MG, Aklillu E, Yasar U, Dahl ML, Spina E, and Ingelman-Sundberg M (2001) Genetic polymorphism of cytochrome P450 2C9 in a Caucasian and a black African population. *Br J Clin Pharmacol* **52**:447–450.
Slobodzian DK, Hsieh JY, and Bayne WF (1985) Simultaneous determination of tranilast and metabolites in plasma and urine using high-performance liquid chromatography. *J Chromatogr* **345**:345–354.
Soars MG, Burchell B, and Riley RJ (2002) In vitro analysis of human drug glucuronidation and prediction of in vivo metabolic clearance. *J Pharmacol Exp Ther* **301**:382–390.
Strassburg CP, Kneip S, Topp J, Obermayer-Straub P, Barut A, Tukey RH, and Manns MP (2000) Polymorphic gene regulation and interindividual variation of UDP-glucuronosyltransferase activity in human small intestine. *J Biol Chem* **275**:36164–36171.
Sullivan-Klose TH, Ghanayem BI, Bell DA, Zhang ZY, Kaminsky LS, Shenfield GM, Miners JO, Birkett DJ, and Goldstein JA (1996) The role of the *CYP2C9*-Leu^{359} allelic variant in the tolbutamide polymorphism. *Pharmacogenetics* **6**:341–349.
Takahashi H, Kashima T, Nomizo Y, Muramoto N, Shimizu T, Nasu K, Kubota T, Kimura S, and Echizen H (1998) Metabolism of warfarin enantiomers in Japanese patients with heart disease having different *CYP2C9* and *CYP2C19* genotypes. *Clin Pharmacol Ther* **63**:519–528.
Watanabe Y, Nakajima M, and Yokoi T (2002) Troglitazone glucuronidation in human liver and intestine microsomes: high catalytic activity of UGT1A8 and UGT1A10. *Drug Metab Dispos* **30**:1462–1469.

Address correspondence to: Dr. Tsuyoshi Yokoi, Drug Metabolism and Toxicology, Division of Pharmaceutical Sciences, Graduate School of Medical Science, Kanazawa University, Kakuma-machi, Kanazawa 920-1192, Japan. E-mail: tyokoi@kenroku.kanazawa-u.ac.jp

THE JOURNAL OF BIOLOGICAL CHEMISTRY VOL. 282, NO. 33, pp. 23996–24003, August 17, 2007

Knock Down of γ-Glutamylcysteine Synthetase in Rat Causes Acetaminophen-induced Hepatotoxicity*

Received for publication, April 3, 2007, and in revised form, June 7, 2007 Published, JBC Papers in Press, June 15, 2007, DOI 10.1074/jbc.M702819200

Sho Akai[‡], Hiroko Hosomi[‡], Keiichi Minami[‡], Koichi Tsuneyama[§], Miki Katoh[‡], Miki Nakajima[‡], and Tsuyoshi Yokoi[‡1]

From the [‡]Division of Pharmaceutical Sciences, Graduate School of Medical Science, Kanazawa University, Kakuma-machi, Kanazawa 920-1192, Japan and [§]Department of Diagnostic Pathology, Graduate School of Medicine and Pharmaceutical Science for Research, University of Toyama, Sugitani 930-0194, Toyama, Japan

Drug-induced hepatotoxicity is mainly caused by hepatic glutathione (GSH) depletion. In general, the activity of rodent glutathione *S*-transferase is 10 to 20 times higher than that of humans, which could make the prediction of drug-induced hepatotoxicity in human more difficult. γ-Glutamylcysteine synthetase (γ-GCS) mainly regulates *de novo* synthesis of GSH in mammalian cells and plays a central role in the antioxidant capacity of cells. In this study, we constructed a GSH-depletion experimental rat model for the prediction of human hepatotoxicity. An adenovirus vector with short hairpin RNA against rat γ-GCS heavy chain subunit (GCSh) (AdGCSh-shRNA) was constructed and used to knock down the GCSh. In *in vitro* study in H4IIE cells, a rat hepatoma cell line, GCSh mRNA and protein were significantly decreased by 80% and GSH was significantly decreased by 50% 3 days after AdGCSh-shRNA infection. In the *in vivo* study in rat, the hepatic GSH level was decreased by 80% 14 days after a single dose of AdGCSh-shRNA (2×10^{11} pfu/ml/body), and this depletion continued for at least 2 weeks. Using this GSH knockdown rat model, acetaminophen-induced hepatotoxicity was shown to be significantly potentiated compared with normal rats. This is the first report of a GSH knockdown rat model, which could be useful for highly sensitive tests of acute and subacute toxicity for drug candidates in preclinical drug development.

Glutathione (5-L-glutamyl-L-cysteinylglycine, GSH)[2] is one of the most abundant tripeptides, consisting of glycine, glutamic acid, and cysteine. It serves an important function in protecting tissues against the degenerating effects of oxidative damage by scavenging free radicals from endogenous or exogenous compounds (1, 2). GSH is synthesized from its precursor amino acids in two steps of enzymatic reactions. γ-Glutamylcysteine synthetase (γ-GCS) (3) catalyzes the formation of γ-glutamylcysteine from glutamic acid and cysteine. GSH synthetase couples glycine to γ-glutamylcysteine to form GSH. γ-GCS is a rate-limiting step in GSH biosynthesis, and GSH is a feedback inhibitor of γ-GCS activity. γ-GCS is a heterodimeric enzyme composed of a catalytic subunit (heavy chain, 73 kDa) (4) and a modulatory subunit (light chain, 27.7 kDa) (5). Studies performed by purified γ-GCS suggested that the active site exists in the catalytic subunit, whereas the modulatory subunit increases the affinity of the catalytic subunit for glutamic acid and decreases the sensitivity to feedback inhibition by GSH (4). In mice, embryos homozygous for the γ-GCS heavy chain (GCSh) mutation fail to gastrulate and die (6). In contrast, homozygous knock-out mice with targeted disruption of the γ-GCS light chain are viable and fertile although the GSH level is decreased by 87% in the liver, and thus this model could be used as a GSH depletion mouse model *in vivo* (7).

Rat is the most frequently used experimental animal for pharmacological and toxicological studies in the drug development process because of their body weight and ease of sampling blood or urine. A standard technique of gene knock out in rat has not been established yet. Recently, a nuclear transfer method has been established and this method may be able to produce conditional knock out and gene replacement in the future (8), but this method is very difficult and not available for general use. Recently, recombinant adenovirus methods are being developed and used for the purpose of clinical therapy or gene delivery *in vivo* (9–11). Furthermore, a small interfering RNA strategy, which has been proven to be more specific and efficient than the full-length antisense cDNA strategy, has been established (12). In addition, an adenovirus-mediated short hairpin RNA (shRNA) knockdown approach could reduce the target gene specifically in the liver in mice, resulting in the expected phenotype (13). However, to our knowledge, there is no report that adenovirus-mediated shRNA knock down was successfully applied in rats *in vivo*. In the present study, we constructed a recombinant adenovirus (AdGCSh-shRNA) that could knock down rat GCSh mRNA efficiently *in vitro* and *in vivo*. We established the GSH-depleted rats and this rat model, when treated with acetaminophen (APAP), which is known to be biotransformed to quinoneimine (14), or some other radical species (15), demonstrated hepatotoxicity with high sensitivity compared with normal rats.

The activity of rodent glutathione *S*-transferase (GST) is about 10 to 20 times higher than that in human (16). Therefore,

* This work was supported in part by Research on Toxicogenomics, Health and Labor Science research grants from the Ministry of Health, Labor, and Welfare of Japan. The costs of publication of this article were defrayed in part by the payment of page charges. This article must therefore be hereby marked "*advertisement*" in accordance with 18 U.S.C. Section 1734 solely to indicate this fact.

[1] To whom correspondence should be addressed: Drug Metabolism and Toxicology, Division of Pharmaceutical Sciences, Graduate School of Medical Science, Kanazawa University, Kakuma-machi, Kanazawa 920-1192, Japan. Tel./Fax: 81-76-234-4407; E-mail: tyokoi@kenroku.kanazawa-u.ac.jp.

[2] The abbreviations used are: GSH, glutathione; GCS, γ-glutamylcysteine synthetase; GCSh, GCS heavy chain; shRNA, short hairpin RNA; APAP, acetaminophen; GAPDH, glyceraldehyde-3-phosphate dehydrogenase; m.o.i., multiplicity of infection; PBS, phosphate-buffered saline; CYP, cytochrome P450; pfu, plaque-forming unit; GST, glutathione S-transferase; AST, aspartate aminotransferase; ALT, alanine aminotransferase.

active metabolites produced *in vivo* in rat would be immediately detoxified by GSH conjugation, which would make the prediction of drug-induced hepatotoxicity in human more difficult. From this perspective, the AdGCSh-shRNA-mediated GSH depletion rat model could be useful for predicting the hepatotoxicity caused by unknown active metabolites of drug candidates produced by Phase I enzymes.

EXPERIMENTAL PROCEDURES

Materials—APAP and GSH were obtained from Wako Pure Chemical Industries (Osaka, Japan). β-NADPH and glutathione reductase were from Oriental Yeast (Tokyo, Japan). ISOGEN was from Nippon Gene (Tokyo, Japan). ReverTra Ace (Moloney Murine Leukemia Virus Reverse Transcriptase RNaseH Minus) was from Toyobo (Tokyo, Japan). The Adenovirus Expression Vector kit (Dual Version), random hexamer and SYBR Premix Ex Taq were from Takara (Osaka, Japan). The QuickTiter Adenovirus Titer Immunoassay kit was from Cell Biolabs (Tokyo, Japan). Lipofectamine 2000 and minimum essential α medium were from Invitrogen. The GeneSilencer shRNA Vector kit was from Gene Therapy Systems (San Diego, CA). Dulbecco's modified Eagle's medium and Ham's F12 medium were from Nissui Pharmaceutical (Tokyo, Japan). All primers and oligonucleotides for shRNA were commercially synthesized at Hokkaido System Sciences (Sapporo, Japan). Standard metabolites of APAP, such as APAP-glucuronide, APAP-sulfate, APAP-mercapturate, APAP-cysteine, and APAP-GSH, were kindly provided by McNeil Consumer Products (Washington, PA). Other chemicals were of analytical grade or the highest commercially available.

Animals—Male Fisher 344 rats (7 weeks old, 130–150 g) were obtained from SLC Japan (Hamamatsu, Japan). Animals were housed in a controlled environment (temperature 25 ± 1 °C, humidity 50 ± 10%, and 12-h light/12-h dark cycle) in the institutional animal facility with access to food and water *ad libitum*. Animals were acclimatized for a week before use for the experiments. Animal maintenance and treatment were conducted in accordance with the National Institutes of Health Guide for Animal Welfare of Japan, as approved by the Institutional Animal Care and Use Committee of Kanazawa University, Japan.

Design of Short Hairpin RNA—Rat GCSh (Gene Bank™ accession code J05181 Gene bank) knock down was achieved by RNA interference using an adenovirus vector-based shRNA approach. The sequences of shRNA-targeted GCSh cDNA were designed by B-Bridge (Mountain View, CA). The sequences of GCSh-shRNA are : top strand, 5′-gatccGTGTGAATGTCCAGAGTTAgaagcttgTAACTCTGGACATTCACACtttttggaagc-3′, and bottom strand, 5′-ggccgcttccaaaaaaGTGTGAATGTCCAGAGTTAcaagcttcTAACTCTGGACATTCACACg-3′. As a negative control, the oligonucleotide sequences of the shRNA target for luciferase from a GeneSilencer shRNA Vector kit were used.

Recombinant Adenovirus—To generate the recombinant adenovirus vector expressing GCSh-shRNA, pGSU6-GFP plasmids were recombined into the pAxcwit using the cosmide-terminal protein complex (COS-TPC) method according to the manufacturer's instruction. In brief, double strand oligo DNA for shRNA of GCSh and luciferase were inserted into the BamHI and NotI sites of the pGSU6-GFP vector. This product was digested by HincII and inserted into the SwaI site of the pAxcwit vector. This pAxcwit vector and the parental adenovirus DNA terminal protein complex were co-transfected into 293 cells by Lipofectamine 2000. The recombinant adenovirus was isolated and propagated into the 293 cells. An adenovirus containing shRNA of GCSh (AdGCSh-shRNA) and one containing shRNA of luciferase (AdLuc-shRNA) were constructed. The titer was determined by a QuickTiter Adenovirus Titer Immunoassay kit. The titers of AdGCSh- or AdLuc-shRNA were 4.95×10^{11} pfu/ml and 2.98×10^{11} pfu/ml, respectively. The viral stock solution was concentrated with the Amicon Ultra-15 filtration system (Millipore, Billerica, MA) for the *in vivo* study.

Cell Culture—The 293 cell line and rat hepatoma cell lines BRL3A and H4IIE were obtained from American Type Culture Collection (Manassas, VA). The human hepatoma cell line HLE was obtained from the Japanese Collection of Research Biosources (Tokyo, Japan). The mouse hepatoma cell line Hepa1–6 was kindly provided by Dr. S. Kaneko (Kanazawa University, Japan). The 293 cell line was maintained in Dulbecco's modified Eagle's medium containing 10% fetal bovine serum (BioWhitaker, Walkersville, MD), 3% glutamine, 16% sodium bicarbonate, and 0.1 mM nonessential amino acids (Invitrogen) in a 5% CO_2 atmosphere at 37 °C. BRL3A cells were maintained in Ham's F12, HLE and Hepa1–6 cells were maintained in Dulbecco's modified Eagle's medium, and H4IIE cells were maintained in α-minimal essential medium. All cell lines were infected by the adenovirus in medium containing 5% fetal bovine serum.

Real-time Reverse Transcription PCR Analysis—RNA from the hepatoma cells or from liver specimens was isolated using ISOGEN. Rat GCSh and glyceraldehyde-3-phosphate dehydrogenase (GAPDH) were quantified by real-time reverse transcription PCR. Primer sequences used in this study were as follows: rat GCSh, 5′-ATG CAGTATTCTGAACTACC-3′ and 5′-ACAAACTCAGATTCACCTAC-3′; mouse GCSh, 5′-TCTAACAAGAAACATCCGGCA-3′ and 5′-GGTCAGGTCGATGTCATTGTA-3′; human GCSh, 5′-ATTAGAAGAAAATCAGGCTC-3′ and 5′-GTAGCCAACTGATCATAAAG-3′; rat GAPDH, 5′-GTTACCAGGGCTGCCTTCTC-3′ and 5′-GGGTTTCCCGTTGATGACC-3′; mouse GAPDH, 5′-TCACCAGGGCTGCCATTTG-3′ and 5′-CTCACCCCATTTGATGTTAGT; human GAPDH, 5′-CCAGGGCTGCTTTTAACTC-3′ and 5′-GCTCCCCCCTGCAAATGA-3′. For the reverse transcription process, total RNA (2 μg) and 150 ng of random hexamer were mixed and incubated at 70 °C for 10 min. RNA solution was added to a reaction mixture containing 100 units of ReverTra Ace, reaction buffer, and 0.5 mM dNTPs in a final volume of 40 μl. The reaction mixture was incubated at 30 °C for 10 min, 42 °C for 1 h, and heated at 98 °C for 10 min to inactivate the enzyme. The real-time PCR was performed using the Smart Cycler (Cepheid, Sunnyvale, CA). PCR mixture contained 1 μl of template cDNA, SYBR Premix Ex Taq solution, and 10 pmol of sense and antisense primers. The PCR condition for GAPDH and GCSh were as follows. After an initial denaturation at 95 °C for 30 s, the amplification was performed by denaturation at 94 °C for 4 s, annealing and extension at 64 °C for

20 s for 45 cycles. Amplified products were monitored directly by measuring the increase of the dye intensity of the SYBR Green I (Molecular Probes, Eugene, OR) that binds to double strand DNA amplified by PCR.

Western Blot Analysis—The H4IIE cell lysates, 1.5 μg, were separated on 10% SDS-polyacrylamide gels and transferred onto polyvinylidene difluoride membrane (Immobilon-P; Millipore). The specific proteins were detected by rabbit anti-human GCSh polyclonal antibody, cross-reacting to rat GCSh (sc-22755; Santa Cruz Biotechnology, Santa Cruz, CA) at a dilution of 1:200. The protein bands were developed by biotinylated second antibody-peroxidase reaction. The quantitative analysis of protein expression was performed using ImageQuant TL Image Analysis software (Amersham Biosciences).

GSH Level—Cell lysates were mixed in 5% (w/v) metaphosphoric acid and incubated on ice for 10 min. After the addition of 0.125 M sodium phosphate buffer containing 6.3 mM EDTA, pH 7.5, the cell lysates were centrifuged at 13,000 × *g* at 4 °C for 5 min. Livers (100 mg) were homogenized with ice-cold 5% sulfosalicylic acid and centrifuged at 8,000 × *g* at 4 °C for 10 min. The GSH concentration in the supernatant was measured as described previously (17).

Adenovirus Infection and APAP Administration in Rats—Fourteen days after one intravenous injection of AdGCSh-shRNA or AdLuc-shRNA at 2×10^{11} pfu/ml/body, the rats were orally administered APAP suspended in 0.5% carboxymethylcellulose (0, 300, 1000 mg/kg body weight). Blood samples were collected at 0, 30, 60, 120, and 180 min after the APAP treatment. Twenty-four hours after the administration of APAP, serum samples were collected for assessment of transaminase levels and for APAP metabolite analysis. The liver was fixed in buffered neutral 10% formalin. The fixed samples were embedded in paraffin and sectioned at a thickness of 2 μm and stained with hematoxylin-eosin for microscopic examination. Rat liver cytosol and microsomes were prepared as described previously (18). In all experiments, the rats were not treated by fasting prior to the APAP treatment or sacrifice.

GST Activity and Cytochrome P450 (CYP) Content—The cytosolic GST activity was determined using 1-chloro-2,4-dinitrobenzene as a substrate according to the method of Habig *et al.* (19). The microsomal cytochrome P450 content was determined by the method of Omura and Sato (20).

Determination of Plasma Concentrations of APAP and Its Metabolites—The plasma concentrations of APAP and its metabolites were measured using a high performance liquid chromatography method described previously (21). In brief, plasma was mixed with an aliquot of acetonitrile containing theophylline as an internal standard. After extraction and centrifugation, the resulting supernatant was evaporated under nitrogen. The residue was diluted with distilled water as necessary before being injected into high performance liquid chromatography. APAP and its metabolites, APAP-GSH, APAP-cysteine, APAP-mercapturate, APAP-glucuronide, and APAP-sulfate, were separated in a Mightysil RP-18 column (4.6 × 150 mm; 5 μm; Kanto Chemical, Tokyo, Japan). APAP and the metabolites, eluted with 1.8% aqueous acetic acid-methanol-H_2O (66:9:100) at a flow rate of 1.0 ml/min, were monitored at 248 nm.

Statistical Analysis—Statistical analyses were performed with the GraphPad Instat version 2.0 computer program (GraphPad Software, San Diego, CA) by Student *t*-test, Dunnett's post hoc test, or Bonferroni test.

RESULTS

Changes of GCSh mRNA Expression and GSH Level in Various Hepatoma Cell Lines—To investigate the knockdown effect on the cells, various hepatoma cells were infected with AdGCSh-shRNA or AdLuc-shRNA (negative control adenovirus) at a multiplicity of infection (m.o.i.) of 20 for 3 days. Real-time reverse transcription PCR analysis and GSH assay were performed to examine the GCSh mRNA expression and GSH suppression (Fig. 1). The expression level of GCSh mRNA was significantly reduced to 20–30% in BRL3A, H4IIE, and Hepa1–6 cells. In contrast, AdGCSh-shRNA was less potent, reducing GCSh mRNA to 45% in HLE cells. The GSH level was suppressed only in H4IIE cells by 50%, despite the efficient GCSh mRNA knock down in BRL3A and Hepa1–6 cells. Based on these results, H4IIE cells were used in the next experiments.

Time-dependent Knockdown Effect of AdGCSh-shRNA in H4IIE Cells—To investigate the most efficient condition for infection, H4IIE cells were infected with AdGCSh-shRNA at m.o.i. 10 or 20 for 1, 2, 3, and 5 days. GCSh mRNA was reduced after 24 h of infection, and an 80% decrease of GCSh mRNA was achieved after 2 days of infection (Fig. 2*A*). The decrease of GCSh mRNA was accompanied by a decrease in GCSh protein (Fig. 2*B*). The GSH level was significantly reduced by 50% after 3 days of AdGCSh-shRNA m.o.i. 20 infection (Fig. 2*C*). There was no difference between 3 and 5 days of infection. These results suggested that a m.o.i. of 20 and 3 days of infection could be an appropriate condition for cytotoxicity experiments.

Effect of APAP Treatment in H4IIE Cells Infected with AdGCSh-shRNA—To investigate the effect of GSH depression on the cytotoxicity of APAP, a 3-(4,5-dimethylthiazol-2-yl)-2,5-diphenyltetrazolium bromide assay was performed. H4IIE cells were infected with AdGCSh-shRNA at m.o.i. 20 or with AdLuc-shRNA in the same conditions as a negative control. After 3 days of infection, H4IIE cells were exposed to various concentrations of APAP of 0, 0.05, 0.1, 0.25, 0.5, 1, 2.5, 5 mM. After 24 h of APAP treatment, AdGCSh-shRNA-infected cells showed no toxic effects compared with control (data not shown).

Infection of AdGCSh-shRNA to Rat—To further investigate *in vivo* in rat, a single tail vein injection to Fisher 344 rats was made to deliver AdGCSh-shRNA. The effects of GCSh knock down were examined 14 days after infection. Control animals were treated with PBS or AdLuc-shRNA. The hepatic GCSh mRNA expression was remarkably decreased dose dependently (Fig. 3*A*). At the dose of 2×10^{11} pfu/ml/body, GCSh mRNA was significantly decreased by 90%. Consistent with the decrease of GCSh mRNA, the hepatic total GSH level was also reduced to 20% at doses above 2×10^{11} pfu/ml/body (Fig. 3*B*). The hepatic GSH level in AdLuc-shRNA-infected rat was slightly increased compared with the PBS-treated rats (Fig. 3*B*).

To examine the hepatotoxic effect of the adenovirus infection, serum AST and ALT were measured 14 days after infection. As shown in Fig. 3*C*, AST was significantly elevated in the

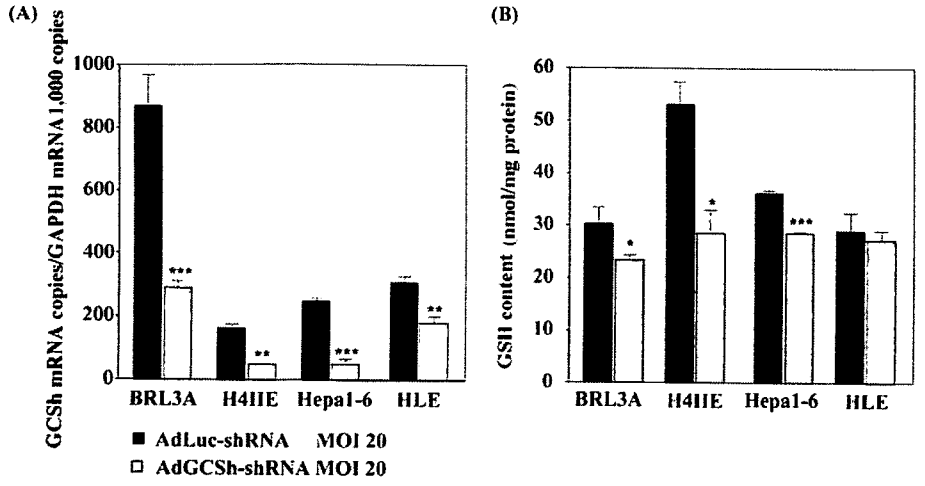

FIGURE 1. **GCSh mRNA expression and the GSH level in various hepatoma cell lines infected with AdGCSh-shRNA.** GCSh mRNA copies/GAPDH mRNA 1,000 copies (*A*) and GSH content (*B*) were determined in each cell 3 days after AdLuc-shRNA or AdGCSh-shRNA infection. Data represent the mean ± S.D. ($n = 3$). *, $p < 0.05$; **, $p < 0.01$; ***, $p < 0.001$ compared with AdLuc-shRNA infected cells.

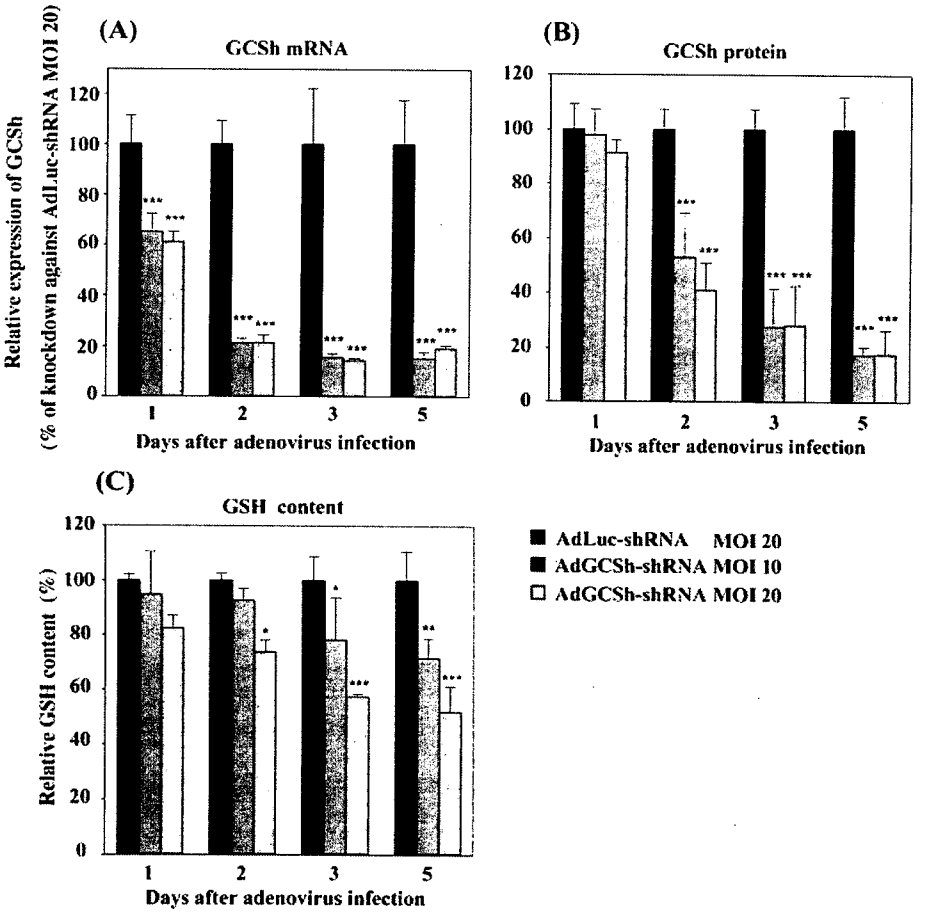

FIGURE 2. **Time-dependent knockdown effect in AdGCSh-shRNA-infected H4IIE cells.** GCSh mRNA (*A*), GCSh protein (*B*), and GSH content (*C*) were determined in H4IIE cells infected with AdLuc-shRNA or AdGCSh-shRNA. GCSh protein was quantified by immunoblotting as described under "Experimental Procedures." Data represent the mean ± S.D. ($n = 3$). *, $p < 0.05$, **, $p < 0.01$, and ***, $p < 0.001$ compared with AdLuc-shRNA-infected cells.

4.0 and 8.0 × 10^{11} pfu/ml/body infection by 1.6- and 4.1-fold, respectively, compared with the control. ALT was significantly elevated in only the 8.0 × 10^{11} pfu/ml/body infection by 2.2-fold compared with the control. The dose of 2.0 × 10^{11} pfu/ml/body did not affect the AST and ALT, and thus this condition was adopted in the next experiments. The cytochrome P450 content and GST activity slightly increased in AdGCSh-shRNA-treated rats (data not shown).

APAP-induced Hepatotoxicity in AdGCSh-shRNA-infected Rat—To determine whether APAP-induced hepatotoxicity was potentiated by the suppression of hepatic GSH, rats were tail vein-injected once with 2.0 × 10^{11} pfu/ml/body AdGCSh-shRNA or AdLuc-shRNA. After 14 days, APAP was orally administered without previous fasting. The serum AST and ALT levels are shown in Figs. 4, *A* and *B*. Twenty-four hours after APAP administration, 300 mg/kg treatment did not result in hepatotoxicity. In contrast, the AdGCSh-shRNA-infected rats treated with 1000 mg/kg APAP demonstrated a significant increase of AST (2159 ± 1156 units/liter) and ALT (924 ± 667 units/liter) compared with AdLuc-shRNA infected rats. Without fasting treatment, the AdLuc-shRNA and normal rats administered 1000 mg/kg APAP did not show hepatotoxicity. The results of the histological examination in 1000 mg/kg APAP-administered rats are shown in Fig. 4*C*. Remarkable hepatic necrosis, especially around the central vein, was observed in AdGCSh-shRNA-treated rats given 1000 mg/kg APAP, consistent with the elevation of AST and ALT. There was no histological change in the other groups.

Metabolism of APAP in Rats Infected with Adenovirus—Changes in the plasma concentration of APAP and its metabolites are shown in Fig. 5. For APAP, APAP-glucuronide, and APAP-sulfate, the maximum plasma concentration was observed 30 min or 1 h after APAP administration. The concentration of APAP-glucuronide was significantly elevated in rats infected with AdGCSh-shRNA compared with AdLuc-shRNA-infected rats (Fig. 5*B*). On the other hand, APAP-sulfate, a major detoxification product in rats generated directly from APAP, was decreased (Fig. 5*C*). For APAP-GSH, APAP-cysteine, and APAP-mercapturate, the maximum plasma concentration was observed 1 h after APAP administration in rats infected with AdGCSh-

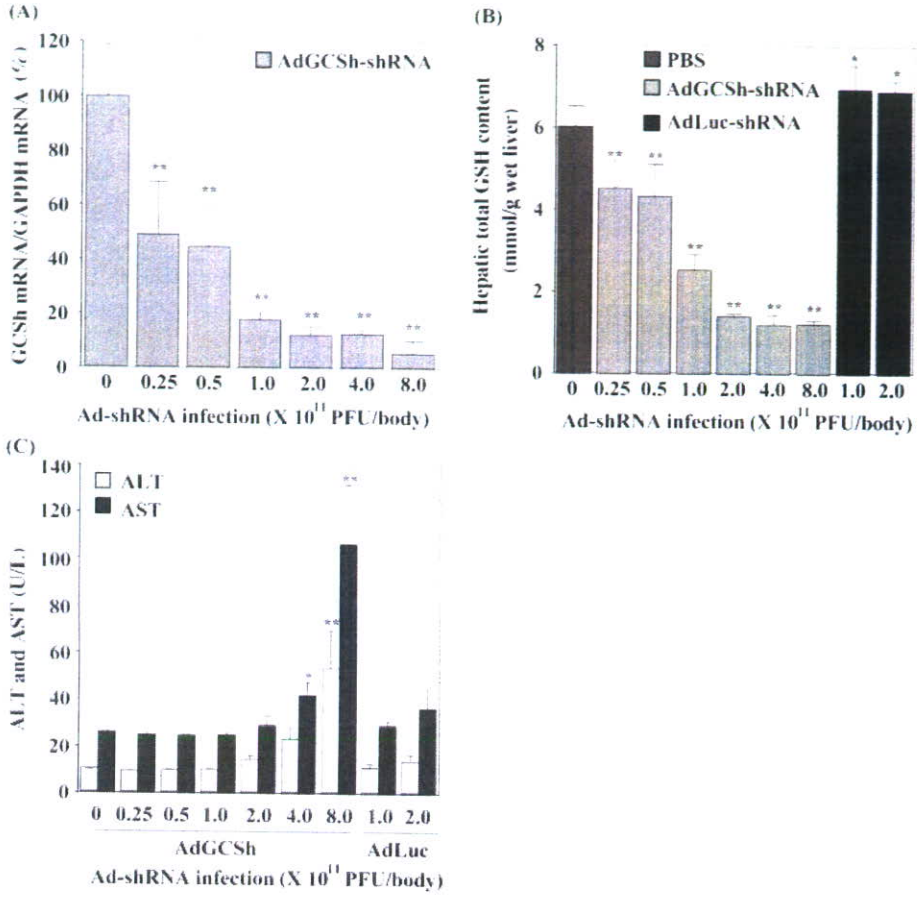

FIGURE 3. **Effects of adenovirus infection on hepatic GCSh mRNA (*A*), GSH level (*B*), ALT and AST (*C*) in rats.** All experiments were performed 14 days after AdGCSh-shRNA or AdLuc-shRNA infection. Data represent the mean ± S.D. ($n = 4$ or 5). *, $p < 0.05$ and **, $p < 0.01$ compared with PBS-treated rats or AdGCSh-shRNA-infected rats.

shRNA. As for the rats infected with AdLuc-shRNA, the concentration of APAP-GSH was gradually decreased, whereas the concentrations of APAP-cysteine and APAP-mercapturate were slightly increased.

Continuation of the Depletion of GSH Level—To examine the continuation of the hepatic GSH depletion, rats were tail vein-injected once with 2×10^{11} pfu/ml/body AdGCSh-shRNA. After 2, 3, 4, and 5 weeks, the hepatic GSH level was measured (Fig. 6). Hepatic GSH was significantly decreased by 80% at 2 to 3 weeks after infection. The hepatic GSH was reduced by 66 and 45% at 4 and 5 weeks after infection, respectively. In addition, at 7 and 10 days after infection of AdGCSh-shRNA, the hepatic GSH was decreased by 20 and 50%, respectively (data not shown). The effects of the circadian rhythm were also examined 2 weeks after infection with AdGCSh-shRNA (data not shown). The hepatic GSH level was lower than those from PBS-treated rats at all the time points examined, and no effect of the circadian rhythm on the GSH level was observed in rats infected with AdGCSh-shRNA.

DISCUSSION

In this study, a recombinant adenovirus vector expressing an shRNA-directed rat GCSh was generated (AdGCSh-shRNA). The GSH level was efficiently decreased by 50% only in H4IIE cells infected with AdGCSh-shRNA (Fig. 1). The target sequence of the rat GCSh is the same as mouse, but it differs from that of human. This would probably affect the mRNA knockdown efficiency. The lack of a decrease of GSH in BRL3A cells may be due to differences in the expression levels of coxsackie and adenovirus receptor (22).

In the cytotoxicity study, APAP treatment did not show a toxic effect in AdGCSh-shRNA-infected cells compared with AdLuc-shRNA-infected cells. APAP is mainly metabolized by UDP-glucuronosyltransferases and sulfotransferases, partly by CYP enzymes (23, 24). APAP toxicity is highly dependent upon bioactivation by CYP enzymes to the reactive intermediate N-acetyl-*p*-benzoquinoneimine (NAPQI), and a depletion of intracellular GSH would cause adduct formation targeting cellular proteins (25–28). A previous report showed that HepG2 cells which stably expressed human CYPs showed cytotoxicity by APAP, but normal HepG2 cells did not (29). H4IIE cells express no CYP enzymes (data not shown), thus APAP would not be metabolized to its toxic metabolite NAPQI and would not cause cytotoxicity.

We successfully produced a GSH-depleted rat model by means of adenovirus-mediated RNA interference technology in order to detect the drug-induced hepatotoxicity with more sensitivity than that provided by normal rats. A previous report described that infection of an adenovirus caused adenovirus-derived hepatotoxicity (30). Therefore, we validated the condition of adenovirus infection (Fig. 3). A significant increase of serum AST and ALT was observed at a high dose of AdGCSh-shRNA (8×10^{11} pfu/ml/body), suggesting adenovirus-derived hepatotoxicity (Fig. 3*C*). On the other hand, doses up to 2×10^{11} pfu/ml/body resulted in no hepatotoxicity and caused GSH depletion by 80% in rat liver. This GSH depletion level is the same as that in GCS light chain knock-out mice (7). Therefore, we determined that a single injection of AdGCSh-shRNA (2×10^{11} pfu/ml/body) was the proper condition for testing the drug-induced hepatotoxicity in this study. Furthermore, the hepatic total P450 content was slightly increased in AdGCSh-shRNA injected rats.

The maximum depletion of GSH was obtained 14 days after infection in rats in the present study, but it was obtained in 5 days in mouse (13). Because there is no previous report of adenovirus-shRNA in rats, this is the first study showing the optimum experimental condition *in vivo* in rats. In regard to the knockdown effect, the GSH level was decreased at most by 50% *in vitro* and 80% *in vivo*. This result may be due to the different

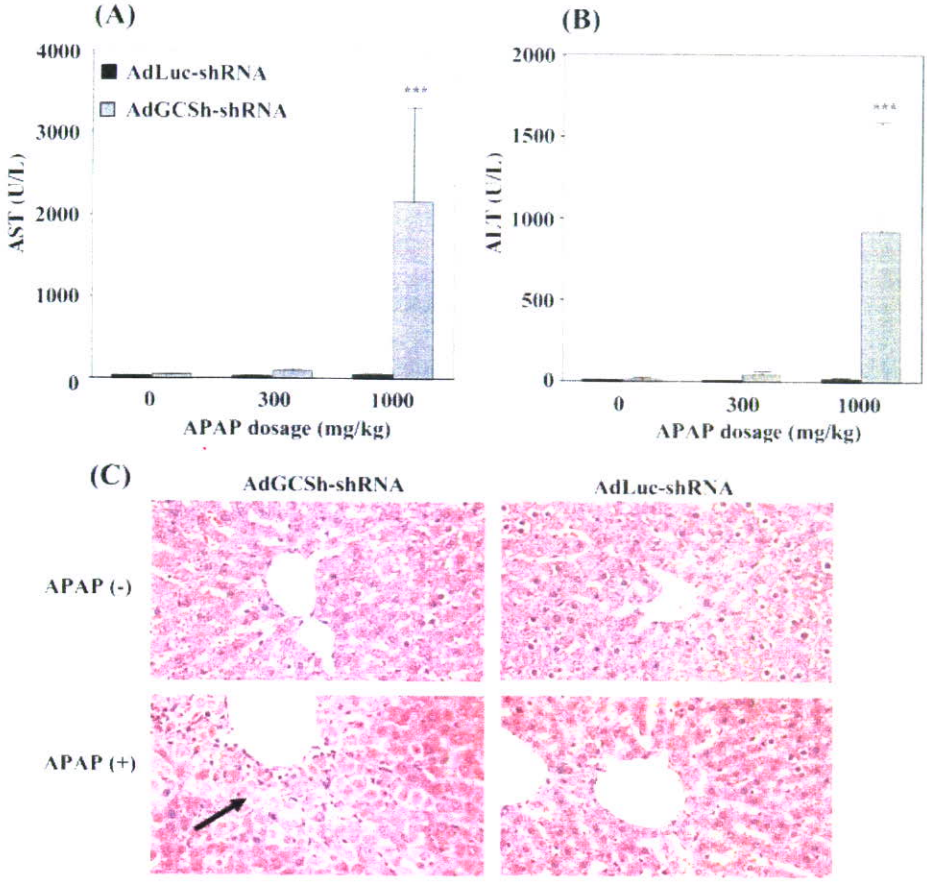

FIGURE 4. **Hepatotoxic effect of APAP in AdGCSh-shRNA-infected rats.** APAP was orally administered without previous fasting. After 24 h, serum AST (*A*) and ALT (*B*) were measured, and hematoxylin-eosin staining (*C*) was performed in sections of rat liver. Hepatic necrosis was observed only in APAP-administered rats infected with AdGCSh-shRNA. *Arrow* indicates areas of hepatic necrosis caused by 1000 mg/kg APAP treatment. Data represent the mean ± S.D. ($n = 4$ or 5). ***, $p < 0.001$ compared with each AdLuc-shRNA-infected group.

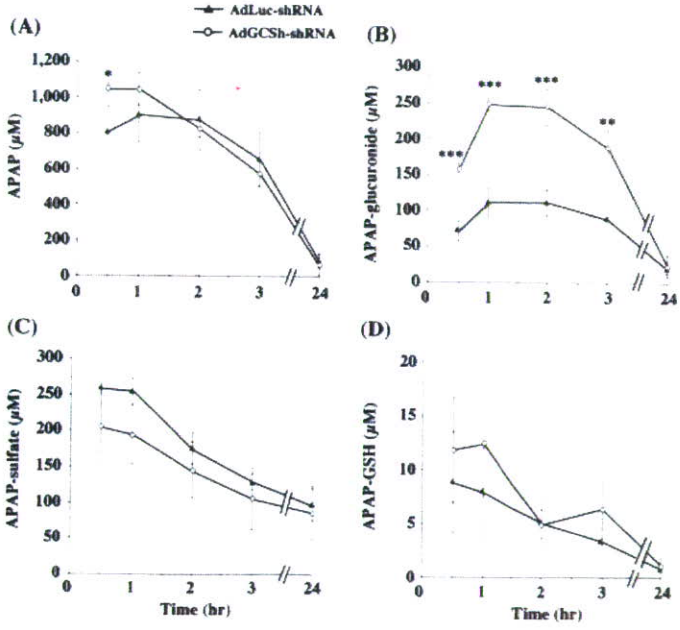

FIGURE 5. **Changes of the plasma concentrations of APAP and its metabolites in rats infected with the adenovirus.** Rats were administered APAP (1000 mg/kg, *p.o.*). Data represent the mean ± S.D. ($n = 3$). *, $p < 0.05$, **, $p < 0.01$, and ***, $p < 0.001$ compared with the AdLuc-shRNA-infected group.

GSH regulation mechanism, which remains to be elucidated in the future.

In previous APAP-induced hepatotoxicity studies, the rats were generally fasted for half or 1 day before drug administration (31–33). In the present study, in order to clarify the involvement of GSH depletion, the rats were not fasted before treatment. APAP-induced hepatotoxicity was observed at a single oral dose of 1000 mg/kg with fasting but was not observed without fasting (data not shown). Previous reports demonstrated that fasting caused a GSH decrease in liver (33, 34). Moreover, transcription of the CYP2E1 gene is potently activated by fasting (35). APAP is metabolized to NAPQI by CYP, mainly by CYP2E1, and thus fasting would cause an overestimation of the APAP-induced hepatotoxicity.

As an *in vivo* hepatotoxicity screening system, a single oral dose of APAP at 300 and 1,000 mg/kg to normal rats with fasting condition was reported by a Pfizer group (36), resulting in no increase of ALT and AST at 300 mg/kg after 24 h of p.o. administration, although a potent increase of ALT and AST in 1,000 mg/kg to normal rats. The same single oral administration of APAP (1,000 mg/kg) with fasting condition was also adapted by the National Toxicogenomics project in Japan as the screening system, resulting in significant increase of ALT and AST at 24 h after treatment (37). However, there is no report about the effect of fasting on APAP hepatotoxicity. In our experiments, without fasting treatment, no hepatotoxicity was observed by single oral administration of 1,000 mg/kg APAP in normal rat, as well as AdGCSh-shRNA-treated rat as shown in Fig. 4. Consequently, in our study, APAP-induced hepatotoxicity was potentiated only in rats with continuously depleted levels of GSH by AdGCSh-shRNA administration, but not by fasting. This indicated that APAP-induced hepatotoxicity would be potentiated only by the GSH depletion.

Infection of AdGCSh-shRNA caused a significant increase of APAP-glucuronide and decrease of APAP-sulfate in the plasma of the rats (Fig. 5), suggesting that GSH depletion caused the induction of UDP-glucuronosyltransferase activity. However, previous reports demonstrated that APAP-glucuronide was a substrate for multidrug resistance-associated protein 2 (MRP2) (38) and that the MRP2 expression level would change depending on the GSH concentration (39). Thus, biliary excretion of APAP-glucuronide would be decreased due to the down-regulation of MRP2 expression, and then the plasma concentration

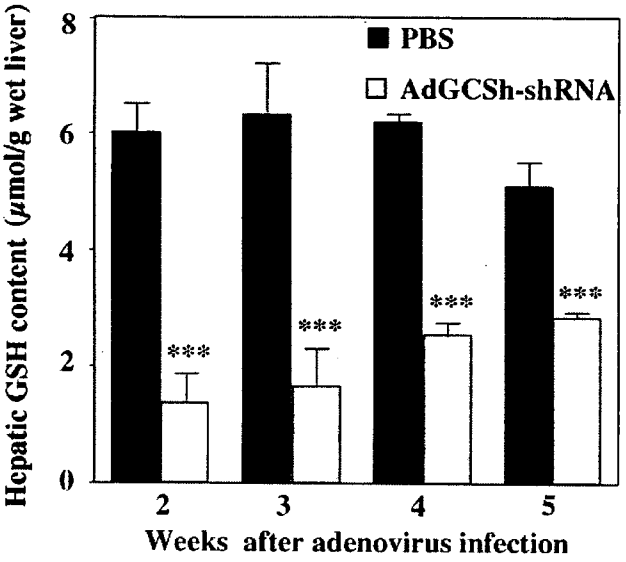

FIGURE 6. **Time-dependent changes of hepatic GSH level in rats infected with AdGCSh-shRNA.** Rat liver was excised at 2, 3, 4, and 5 weeks after infection with AdGCSh-shRNA. Data represent the mean ± S.D. (n = 3 to 5). ***, $p < 0.001$ compared with the PBS-treated group.

of APAP-glucuronide would be increased. The APAP-sulfate showed a tendency of decrease; however, the mechanism remains to be elucidated. The plasma concentrations of APAP-GSH, APAP-cysteine, and APAP-mercapturate were increased in rats infected with AdGCSh-shRNA a short time after APAP administration. The GSH depletion in liver caused by AdGCSh-shRNA slightly induced GST activity, which might be the reason for the slightly increased plasma concentrations of APAP-GSH, APAP-cysteine, and APAP-mercapturate.

Because a recombinant adenovirus is delivered predominantly to liver (40), GSH would not be reduced in other organs. However, a recent report demonstrated that a single tail vein adenovirus injection caused extra-hepatic tissue infection and expression of the target gene, especially in spleen, heart, and lung (41). Based on this report, GSH was examined in extra-hepatic tissue in the present study, but no decrease of the GSH level was observed (data not shown).

The role of GSH in the hepatotoxicity of APAP is very complex (42). Mouse lacking GST Pi was reported as showing resistance to APAP hepatotoxicity, as well as significant increased level of hepatic GSH (43). For such kind of *in vivo* hepatotoxicity studies, the present GSH knockdown system would be very useful.

Homozygous embryonic mice with targeted disruption of GCSh have been produced, but they are not viable because they fail to gastrulate (6). To generate a GSH depletion model from the perspective of gene recombination, GCS light chain knockout mice were produced that were viable and fertile and had no overt phenotype (7). Although the GSH depletion mouse model would be helpful for preclinical drug development, rats are easier to handle and scientifically reliable. Therefore, genetically modified rats are needed for further investigation. In conclusion, a hepatic GSH knockdown rat model was established for the first time in this study. To our knowledge, this is the first report demonstrating that a lethal gene was efficiently depleted by adenovirus-mediated RNA interference in rat. This rat model could be useful as a highly sensitive drug-induced hepatotoxicity test for drug candidates in preclinical drug development.

Acknowledgment—We thank Brent Bell for reviewing the manuscript.

REFERENCES

1. Reed, D. J. (1986) *Biochem. Pharmacol.* **35,** 7–13
2. Lu, S. C. (1999) *FASEB J.* **13,** 1169–1183
3. Meister, A., and Anderson, M. E. (1983) *Annu. Rev. Biochem.* **52,** 711–760
4. Huang, C. S., Chang, L. S., Anderson, M. E., and Meister, A. (1993) *J. Biol. Chem.* **268,** 19675–19680
5. Huang, C. S., Anderson, M. E., and Meister, A. (1993) *J. Biol. Chem.* **268,** 20578–20583
6. Shi, Z. Z., Osei-Frimpong, J., Kala, G., Kala, S. V., Barrios, R. J., Habib, G. M., Lukin, D. J., Danney, C. M., Matzuk, M. M., and Lieberman, M. W. (2000) *Proc. Natl. Acad. Sci. U. S. A.* **97,** 5101–5106
7. Yang, Y., Dieter, M. Z., Chen, Y., Shertzer, H. G., Nebert, D. W., and Dalton, T. P. (2002) *J. Biol. Chem.* **277,** 49446–49452
8. Zhou, Q., Renard, J. P., Le Friec, G., Brochard, V., Beaujean, N., Cherifi, Y., Fraichard, A., and Cozzi, J. (2003) *Science* **302,** 1179
9. Peng, Z. C. (2005) *Hum. Gene Ther.* **16,** 1016–1027
10. Chu, R. L., Post, D. E., Khuri, F. R., and Van Meir, E. G. (2004) *Clin. Cancer Res.* **10,** 5299–5312
11. Kruyt, F. A., and Curiel, D. T. (2002) *Hum. Gene Ther.* **13,** 485–495
12. Meister, G., and Tuschl, T. (2004) *Nature* **431,** 343–349
13. Xu, H., Wilcox, D., Nguyen, P., Voorbach, M., Suhar, T., Morgan, S. J., An, W. F., Ge, L., Green, J., and Wu, Z. (2006) *Biochem. Biophys. Res. Commun.* **349,** 439–448
14. Dahlin, D. C., Miwa, G. T., Lu, A. Y., and Nelson, S. D. (1984) *Proc. Natl. Acad. Sci. U. S. A.* **81,** 327–331
15. Moldeus, P., Andersson, B., Rahimtula, A., and Berggren, M. (1982) *Biochem. Pharmacol.* **31,** 1363–1368
16. Grover, P. L., and Sims, P. (1964) *Biochem. J.* **90,** 603–606
17. Tietze, F. (1969) *Anal. Biochem.* **27,** 502–522
18. Guengerich, F. P., Shimada, T., Yun, C. H., Yamazaki, H., Raney, K. D., Their, R., Coles, B., and Harris, T. M. (1994) *Environ. Health Perspect.* **102,** (Suppl.) 49–53
19. Habig, W. H., Pabst, M. J., and Jakoby, W. B. (1974) *J. Biol. Chem.* **249,** 7130–7139
20. Omura, T., and Sato, R. (1964) *J. Biol. Chem.* **239,** 2370–2378
21. Kim, Y. C., and Lee, S. J. (1998) *Toxicology* **128,** 53–61
22. Huang, K. C., Altinoz, M., Wosik, K., Larochelle, N., Koty, Z., Zhu, L., Holland, P. C., and Nalbantoglu, J. (2005) *Int. J. Cancer* **113,** 738–745
23. Howie, D., Adriaenssens, P., and Prescott, L. F. (1977) *J. Pharm. Pharmacol.* **29,** 235–237
24. Tone, Y., Kawamata, K., Murakami, T., Higashi, Y., and Yata, N. (1990) *J. Pharmacobio-dyn* **13,** 327–335
25. Miner, D. J., and Kissinger, P. T. (1979) *Biochem. Pharmacol.* **28,** 3285–3290
26. Hinson, J. A., Pohl, L. R., Monks, T. J., and Gillette, J. R. (1981) *Life Sci.* **29,** 107–116
27. Albano, E., Rundgren, M., Harvison, P. J., Nelson, S. D., and Moldeus, P. (1985) *Mol. Pharmacol.* **28,** 306–311
28. van de Straat, R., Vromans, R. M., Bosman, P., de Vries, J., and Vermeulen, N. P. (1988) *Chem. Biol. Interact.* **64,** 267–280
29. Yoshitomi, S., Ikemoto, K., Takahashi, J., Miki, H., Namba, M., and Asahi, S. (2001) *Toxicol. In Vitro* **3,** 245–256
30. Callahan, S. M., Boquet, M. P., Ming, X., Brunner, L. J., and Croyle, M. A. (2006) *J. Gene Med.* **8,** 566–576
31. Merrick, B. A., Bruno, M. E., Madenspacher, J. H., Wetmore, B. A., Foley, J., Pieper, R., Zhao, M., Makusky, A. J., McGrath, A. M., and Zhou, J. X. (2006) *J. Pharmacol. Exp. Ther.* **318,** 792–802
32. Kim, Y. W., Ki, S. H., Lee, J. R., Lee, S. J., Kim, C. W., Kim, S. C., and Kim, S. G. (2006) *Chem. Biol. Interact.* **161,** 125–138
33. Pessayre, D., Wandscheer, J. C., Cobert, B., Level, R., Degott, C., Batt, A. M., Martin, N., and Benhamou, J. P. (1980) *Biochem. Pharmacol.* **29,**

2219–2223
34. Jaeschke, H., and Wendel, A. (1985) *Biochem. Pharmacol.* **34,** 1029–1033
35. Johansson, I., Lindros, K. O., Eriksson, H., and Ingelman-Sundberg, M. (1990) *Biochem. Biophys. Res. Commun.* **173,** 331–338
36. Kikkawa, R., Fujikawa, M., Yamamoto, T., Hamada,Y., Yamada, H., and Horii, I. (2006) *J. Toxicol. Sci.* **31,** 23–34
37. Morishita, K., Mizukawa, Y., Kasahara, T., Okuyama, M., Takashima, K., Toritsuka, N., Miyagishima, T., Nagao, T., and Urushidani, T. (2006) *J. Toxicol. Sci.* **31,** 491–507
38. Xiong, H., Turner, K. C., Ward, E. S., Jansen, P. L., and Brouwer, K. L. (2000) *J. Pharmacol. Exp. Ther.* **295,** 512–518
39. Sekine, S., Ito, K., and Horie, T. (2006) *Free Radic. Biol.* **40,** 2166–2174
40. Hayder, H., Blanden, R. V., Korner, H., Riminton, D. S., Sedgwick, J. D., and Mullbacher, A. (1999) *J. Immunol.* **163,** 1516–1520
41. Crettaz, J., Berraondo, P., Mauleon, I., Ochoa, L., Shankar, V., Barajas, M., van Rooijen, N., Kochanek, S., Qian, C., and Prieto, J. (2006) *Hepatology* **44,** 623–632
42. Farkas, D., and Tannenbaum, S. R. (2005) *Curr. Drug Metab.* **6,** 111–125
43. Henderson, C. J., Wolf, C. R., Kitteringham, N., Powell, H., and Park, B. K. (2000) *Proc. Natl. Acad. Sci. U. S. A.* **97,** 12741–12745

0090-9556/07/3503-335–339$20.00
DRUG METABOLISM AND DISPOSITION
Vol. 35, No. 3
11064/3183027
Printed in U.S.A.

DMD 35:335–339, 2007

Short Communication

CYP2A13 Metabolizes the Substrates of Human CYP1A2, Phenacetin, and Theophylline

Received October 24, 2006; accepted December 15, 2006

ABSTRACT:

Human cytochrome CYP2A13 shows overlapping substrate specificity with CYP2A6, catalyzing the metabolism of coumarin, nicotine, cotinine, and 4-(methylnitrosamino)-1-(3-pyridyl)-1-butanone. Recently, it was found that CYP2A13 could catalyze the metabolic activations of 4-aminobiphenyl and aflatoxin B_1, which are known to be catalyzed by human CYP1A2. In the present study, we investigated the substrate specificity of CYP2A13. It was shown that CYP2A13 could catalyze ethoxyresorufin *O*-deethylation, methoxyresorufin *O*-demethylation, and phenacetin *O*-deethylation, which are used as marker activities for human CYP1A2. Although the intrinsic clearances (V_{max}/K_m) of the two former reactions by CYP2A13 were much lower than that of CYP1A2, the value of the last reaction by CYP2A13 was 2-fold higher than that of CYP1A2. Of particular interest was that CYP2A13 has higher affinity toward phenacetin than CYP1A2. In contrast, CYP2A6 hardly catalyzed these reactions, although the amino acid identity with CYP2A13 is as high as 93.5%. Furthermore, we found that CYP2A13 can catalyze theophylline 8-hydroxylation and 3-demethylation, which are known to be mainly catalyzed by human CYP1A2, although the intrinsic clearances were approximately one-tenth that of CYP1A2. CYP2A13 would not contribute to the systemic clearance of these drugs because CYP2A13 is hardly expressed in human liver. However, it may play a role in metabolism in local tissues such as lung or trachea. In conclusion, the results of the present study could extend our understanding of the substrate specificity of CYP2A13.

The human *CYP2A* gene subfamily comprises two functional genes, *CYP2A6* (Yamano et al., 1990) and *CYP2A13* (Su et al., 2000), and a nonfunctional gene, *CYP2A7* (Yamano et al., 1990). CYP2A6 is mainly expressed in the liver, whereas CYP2A13 is predominantly expressed in the respiratory tract, with the highest level in the nasal mucosa, followed by the lung and trachea (Koskela et al., 1999; Gu et al., 2000; Su et al., 2000). Both CYP2A6 and CYP2A13 are composed of 494 amino acids with a high degree of identity (93.5%). CYP2A6 is involved in the metabolism of coumarin and nicotine and the metabolic activation of tobacco-specific nitrosamines such as 4-(methylnitrosamino)-1-(3-pyridyl)-1-butanone (Yamano et al., 1990; Tiano et al., 1993; Nakajima et al., 1996). CYP2A13 is also active toward these CYP2A6 substrates (Su et al., 2000; von Weymarn and Murphy, 2003; Bao et al., 2005). Although CYP2A13 is less active for coumarin 7-hydroxylation than CYP2A6, it is much more active for nicotine, cotinine, and especially 4-(methylnitrosamino)-1-(3-pyridyl)-1-butanone metabolisms (Su et al., 2000; He et al., 2004; Bao et al., 2005). Thus, although there are distinct overlaps in the substrate specificities of CYP2A6 and CYP2A13, the catalytic efficiencies differ between the two isoforms.

Recently, we found that CYP2A13 could catalyze the metabolic activation of 4-aminobiphenyl (Nakajima et al., 2006). Furthermore, it has been reported that CYP2A13 is active for the metabolism of aflatoxin B_1 (He et al., 2006). In contrast, CYP2A6 is not active for these substrates. These activities had been known to be catalyzed by CYP1A2 (Gallagher et al., 1996; Hammons et al., 1997). In the present study, we investigated whether CYP2A13 has the ability to metabolize the compounds that are representative substrates of CYP1A2.

T.F. was supported as a Research Fellow of the Japan Society for the Promotion of Science.

Article, publication date, and citation information can be found at http://dmd.aspetjournals.org.

doi:10.1124/dmd.106.011064.

Materials and Methods

Chemicals. Coumarin, 7-hydroxycoumarin, acetaminophen, theophylline, 1-methylxanthine (1-MX), 3-methylxanthine (3-MX), 1,3-dimethyluric acid (1,3-DMU), and theobromine were obtained from Wako Pure Chemicals (Osaka, Japan). Phenacetin, ethoxyresorufin, methoxyresorufin, and resorufin were from Sigma-Aldrich (St. Louis, MO). All the other chemicals and solvents were of analytical grade or the highest grade commercially available.

Enzyme Preparations. *Escherichia coli* membranes expressing recombinant human CYP1A1/NPR (Yamazaki et al., 2002), CYP1A2/NPR (Yamazaki et al., 2002), CYP2A6/NPR (Fukami et al., 2004), and CYP2A13/NPR (Yamanaka et al., 2005) were previously prepared in our laboratory. The cytochrome P450 (P450) content and protein concentration were determined according to a method described previously (Omura and Sato, 1964; Bradford, 1976). NADPH-cytochrome *c* reductase activity was determined as described previously (Williams and Kamin, 1962; Yasukochi and Masters, 1976) using $\Delta_{\varepsilon 550}$ = 21.1 mM/cm, and the content was calculated using the specific activity of 3.0 μmol reduced cytochrome *c*/min/nmol NPR based on purified rabbit NPR preparations (Parikh et al., 1997).

Enzyme Assays. Coumarin 7-hydroxylation was determined as described previously (Ohyama et al., 2000). The substrate concentration was 0.1 to 5 μM. Ethoxyresorufin *O*-deethylation and methoxyresorufin *O*-demethylation were determined as described previously (Nakajima et al., 1998). The concentrations of ethoxyresorufin and methoxyresorufin were 0.1 to 2.5 μM for CYP1A1 and CYP1A2 or 0.5 to 7.5 μM for CYP2A6 and CYP2A13.

ABBREVIATIONS: 1-MX, 1-methylxantine; 3-MX, 3-methylxantine; 1,3-DMU, 1,3-dimethyluric acid; P450, cytochrome P450; HPLC, high-performance liquid chromatography.

Phenacetin *O*-deethylation was determined as follows: a typical incubation mixture (final volume of 0.2 ml) contained the *E. coli* membrane preparation (5 pmol of P450), 100 mM potassium phosphate buffer (pH 7.4), an NADPH-generating system (0.5 mM $NADP^+$, 5 mM glucose 6-phosphate, 5 mM $MgCl_2$, and 1 U/ml glucose-6-phosphate dehydrogenase), and 10 to 250 μM phenacetin. The reaction was initiated by the addition of the NADPH-generating system after 2-min preincubation at 37°C. After the 20-min incubation at 37°C, the reaction was terminated by the addition of 10 μl of 60% perchloric acid. After the removal of protein by centrifugation at 10,000 rpm for 5 min, a 20-μl portion of the supernatant was subjected to high-performance liquid chromatography (HPLC). HPLC analyses were performed using an L-7100 pump (Hitachi, Tokyo, Japan), L-7200 autosampler (Hitachi), and a D-2500 integrator (Hitachi) equipped with a Mightysil RP-18 C18 GP (4.6 × 150 mm, 5 μm) column (Kanto Chemical, Tokyo, Japan). The eluent was monitored at 245 nm. The mobile phase was 8% acetonitrile containing 50 mM potassium phosphate (pH 4.2). The flow rate was 1.0 ml/min. The column temperature was 35°C. The quantification of acetaminophen was performed by comparing the HPLC peak height with that of an authentic standard.

Theophylline demethylation and hydroxylation were determined as follows: a typical incubation mixture (final volume of 0.5 ml) contained an *E. coli* membrane preparation (5 pmol of P450), 100 mM potassium phosphate buffer (pH 7.4), an NADPH-generating system, and 0.1 to 125 mM theophylline. The reaction was initiated by the addition of the NADPH-generating system after 2-min preincubation at 37°C. After the 30-min incubation at 37°C, the reaction was terminated by the addition of 25 μl of 1 M hydroxychloride. Theobromine (250 pmol) was added as an internal standard. The reaction mixture was extracted with 5 ml of dichloromethane/isopropyl alcohol (75:25 v/v) and then centrifuged at 2000 rpm for 10 min to separate the aqueous and organic fractions. The organic fraction was evaporated under a gentle stream of nitrogen at 40°C. The residue was redissolved in 100 μl of mobile phase, and then the 50-μl portion of the sample was subjected to HPLC. The HPLC apparatus was the same as described above except for a Mightysil RP-18 C18 GP Aqua (4.6 × 150 mm, 5 μm) column (Kanto Chemical). The eluent was monitored at 274 nm with a noise-base clean Uni-3 (Union, Gunma, Japan). The mobile phase was 2.5% methanol containing 10 mM sodium acetate (pH 4.5). The flow rate was 1.0 ml/min (0–23 min) and 1.5 ml/min (24–39 min). The column temperature was 35°C. Quantification of the metabolites was performed by comparing the HPLC peak height ratios with that of authentic standards with reference to an internal standard.

Data Analysis. Kinetic parameters were estimated from the fitted curve using a computer program designed for nonlinear regression analysis (KaleidaGraph, Synergy Software, Reading, PA). All the data were analyzed using the mean of duplicated determinations. Data are mean ± S.D. of three independent experiments. Statistical analyses of the kinetic parameters were performed using the two-tailed Student's *t* test. A value of $P < 0.05$ was considered statistically significant.

Results

Coumarin 7-Hydroxylation. To confirm that recombinant CYP2A13 expressed in *E. coli*, which we constructed, is enzymatically active, the coumarin 7-hydroxylase activity was measured. The K_m and V_{max} values by CYP2A13 were 0.7 ± 0.0 μM and 1.7 ± 0.1 pmol/min/pmol P450, respectively. The K_m and V_{max} values in CYP2A6 were 1.3 ± 0.2 μM and 5.0 ± 0.8 pmol/min/pmol P450, respectively. The intrinsic clearance (V_{max}/K_m) of CYP2A13 (2.6 ± 0.1 μl/min/pmol P450) was lower than that of CYP2A6 (3.8 ± 0.7 μl/min/pmol P450).

Ethoxyresorufin *O*-Deethylation and Methoxyresorufin *O*-Demethylation. Using the recombinant CYP2A13, the ethoxyresorufin *O*-deethylase activity and methoxyresorufin *O*-demethylase activity were measured. CYP2A13 exhibited both activities, although the activities were inconsiderable compared with CYP1A1 or CYP1A2. In contrast, CYP2A6 did not show detectable activities. The kinetics by CYP2A13, CYP1A1, and CYP1A2 were fitted to the Michaelis-Menten equation (Fig. 1, A and B). For the ethoxyresorufin *O*-deethylation, the K_m and V_{max} values of CYP2A13 were higher and lower, respectively, than those of CYP1A1 and CYP1A2, resulting in conspicuously lower intrinsic clearance of CYP2A13 than those of CYP1A1 and CYP1A2 (Table 1). Similarly, the intrinsic clearance of CYP2A13 for the methoxyresorufin *O*-demethylation was also lower than those of CYP1A1 and CYP1A2 (Table 1). Thus, CYP2A13 showed slight activities for ethoxyresorufin *O*-deethylation and methoxyresorufin *O*-demethylation.

Phenacetin *O*-Deethylation. We determined whether CYP2A13 catalyzes phenacetin *O*-deethylation, which is known as a typical activity for CYP1A2 (Sesardic et al., 1988). Surprisingly, CYP2A13 showed higher activity for phenacetin *O*-deethylation than CYP1A2 (Fig. 1C). In contrast, CYP2A6 showed scarce activity (0.03 pmol/min/pmol P450) only at a high substrate concentration (250 μM); therefore, the kinetic parameters could not be calculated. The K_m and V_{max} values of CYP2A13 were lower and higher, respectively, than those of CYP1A1 and CYP1A2 (Table 2), resulting in higher intrinsic clearance of CYP2A13 than that of CYP1A2 (2-fold) and CYP1A1 (5-fold).

Theophylline Metabolism. Theophylline is mainly metabolized to three metabolites, 1,3-DMU, 1-MX, and 3-MX by P450s, mainly CYP1A2 in human liver. It has been reported that human lung microsomes can also convert theophylline to 1,3-DMU (Bowen et al., 1991). Because CYP2A13 is highly expressed in the human respiratory tract, we determined whether CYP2A13 is able to metabolize theophylline. As shown in Fig. 1, D and E, CYP2A13 showed metabolic activities for theophylline 8-hydroxylation (1,3-DMU formation) and 3-demethylation (1-MX formation). Interestingly, CYP2A6 also showed activity for theophylline 8-hydroxylation. CYP2A13 showed moderate intrinsic clearance for 8-hydroxylation, following CYP1A2 (Table 3). Although the intrinsic clearance of CYP2A13 was one-tenth that of CYP1A2, it was higher than that of CYP2A6 and CYP1A1. The intrinsic clearance of CYP2A13 for theophylline 3-demethylation was one-sixth that of CYP1A2. Theophylline 1-demethylation (3-MX formation) was detected only by CYP1A2.

Discussion

The *CYP2A13* gene was first cloned in 1995 (Fernandez-Salguero et al., 1995), and the expression of CYP2A13 mRNA in human tissues was determined in 1999 (Koskela et al., 1999). Before 2000, the CYP2A13 protein was assumed to be nonfunctional based on its sequence features of CYP2A13 that resemble the nonfunctional CYP2A7. However, the fact that CYP2A13 is a functional enzyme was first shown by constructing heterologously expressed CYP2A13 in baculovirus-infected insect cells (Su et al., 2000). They reported that CYP2A13 could catalyze coumarin 7-hydroxylation but was much less active than CYP2A6 (0.26 versus 2.2 pmol/min/pmol P450 at 100 μM coumarin concentration). von Weymarn and Murphy (2003) subsequently reported that the K_m and V_{max} values of coumarin 7-hydroxylation by recombinant CYP2A13 in baculovirus-infected insect cells were 0.48 μM and 0.15 pmol/min/pmol P450, respectively. Similarly, He et al. (2004) reported that K_m and V_{max} values by the recombinant CYP2A13 in baculovirus-infected insect cells were 2.2 μM and 0.69 pmol/min/pmol P450, respectively. Thus, the kinetic parameters for coumarin 7-hydroxylation by CYP2A13 obtained in the present study were similar to those of previous results.

Ethoxyresorufin *O*-deethylation, methoxyresorufin *O*-demethylation, and phenacetin *O*-deethylation are used as marker activities for CYP1A2 (Eugster et al., 1993; Tassaneeyakul et al., 1993). Interestingly, the data presented here showed that CYP2A13 could catalyze these reactions. Of particular interest is that CYP2A13 showed higher activity for phenacetin *O*-deethylation than CYP1A2. In contrast to CYP2A13, CYP2A6 hardly catalyzes phenacetin *O*-deethylation. Pre-

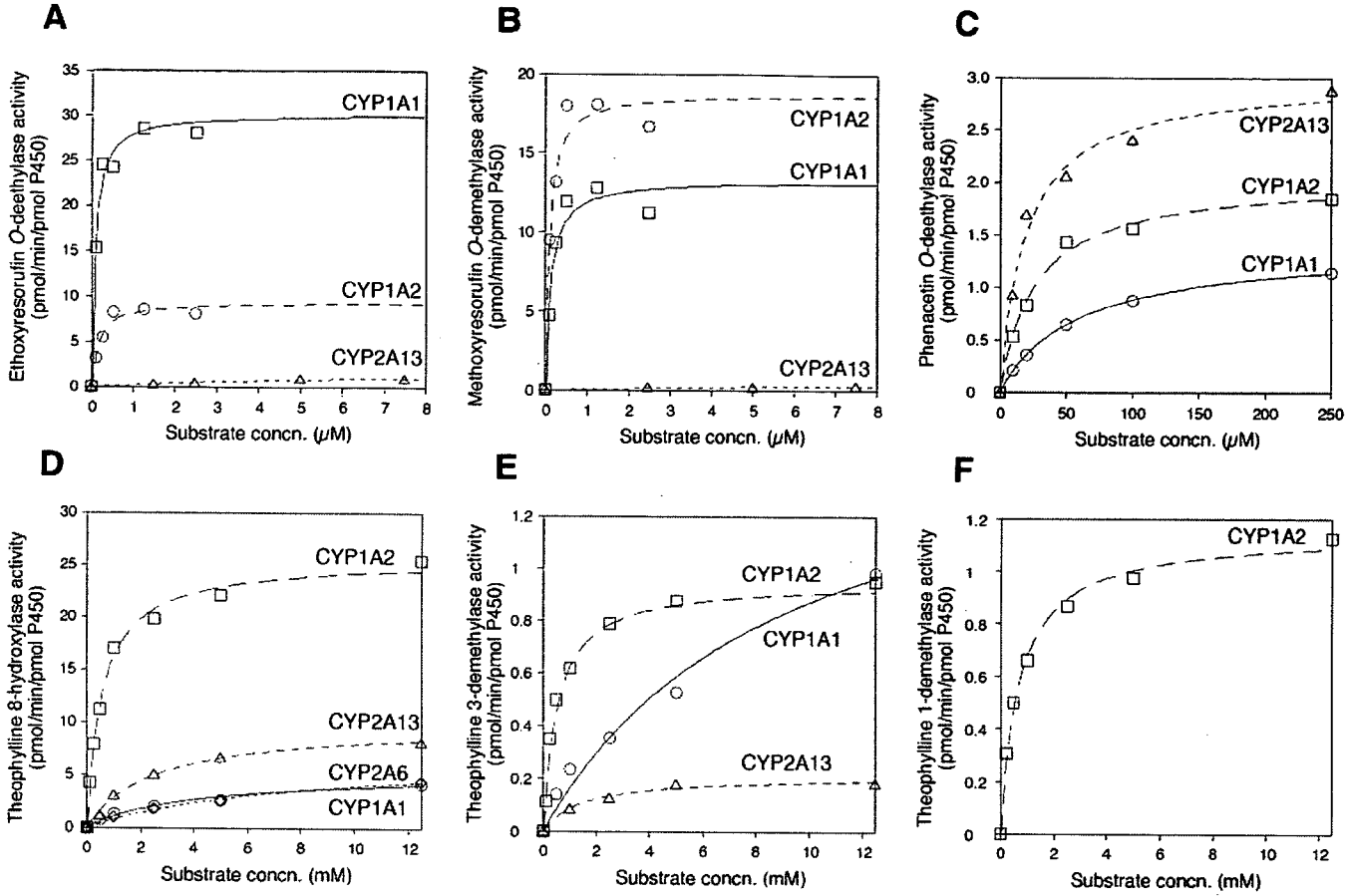

FIG. 1. Kinetic analyses of ethoxyresorufin *O*-deethylation (A), methoxyresorufin *O*-demethylation (B), phenacetin *O*-deethylation (C), theophylline metabolism (D, 8-hydroxylation; E, 3-demethylation; F, 1-demethylation) catalyzed by recombinant CYP1A1, CYP1A2, CYP2A6, and CYP2A13 expressed in *E. coli*. The kinetic parameters were estimated from the fitted curve using the computer program KaleidaGraph designed for nonlinear regression analysis. Each point represents the mean of duplicate determinations.

TABLE 1

Kinetic parameters for ethoxyresorufin O-deethylation and methoxyresorufin O-demethylation by recombinant CYP1As and CYP2As

Data are mean ± S.D. of three independent experiments.

	K_m	V_{max}	V_{max}/K_m
	μM	*pmol/min/pmol P450*	*μl/min/pmol P450*
Ethoxyresorufin *O*-deethylation			
CYP1A1	0.1 ± 0.0	33.5 ± 1.4	321.8 ± 5.2
CYP1A2	0.2 ± 0.0	10.4 ± 1.9	65.7 ± 6.1
CYP2A6	N.D.	N.D.	N.D.
CYP2A13	7.2 ± 1.5[a,b]	2.1 ± 0.3[a,b]	0.3 ± 0.0[a,b]
Methoxyresorufin *O*-demethylation			
CYP1A1	0.1 ± 0.0	13.3 ± 2.1	103.5 ± 11.8
CYP1A2	0.1 ± 0.0	19.9 ± 0.5	177.0 ± 27.5
CYP2A6	N.D.	N.D.	N.D.
CYP2A13	5.9 ± 3.5[a,b]	0.5 ± 0.1[a,b]	0.1 ± 0.0[a,b]

N.D.. not detected.
[a] $P < 0.005$ compared with CYP1A1.
[b] $P < 0.005$ compared with CYP1A2.

TABLE 2

Kinetic parameters for phenacetin O-deethylation by recombinant CYP1As and CYP2As

Data are mean ± S.D. of three independent experiments.

	K_m	V_{max}	V_{max}/K_m
	μM	*pmol/min/pmol P450*	*nl/min/pmol P450*
CYP1A1	56.2 ± 2.3	1.5 ± 0.1	26.8 ± 2.7
CYP1A2	29.2 ± 0.4	1.9 ± 0.1	66.4 ± 4.2
CYP2A6	N.A.	N.A.	N.A.
CYP2A13	21.8 ± 2.4[a,b]	2.9 ± 0.3[a,b]	133.2 ± 17.6[a,c]

N.A., not applicable.
[a] $P < 0.005$ compared with CYP1A1.
[b] $P < 0.05$ and [c] $P < 0.005$ compared with CYP1A2.

viously, Venkatakrishnan et al. (1998) reported that the K_m value of CYP2A6 for phenacetin *O*-deethylation was 4098 μM. Thus, phenacetin is a substrate of CYP2A13, but not CYP2A6, even though the amino acid identity between the two enzymes is as high as 93.5%. Rabbit CYP2A isoforms, CYP2A10 and CYP2A11, have been reported to catalyze phenacetin *O*-deethylation (Peng et al., 1993). These isoforms show higher amino acid identity to CYP2A13 rather than CYP2A6, as regards 32 amino acids showing differences between CYP2A6 and CYP2A13 (22 of 32 amino acids correspond to CYP2A13, whereas only 5 of 32 amino acids correspond to CYP2A6). Therefore, these subtle changes in amino acids may contribute to determining the substrate specificity toward phenacetin.

Theophylline is used to manage bronchial asthma and chronic obstructive pulmonary disease. Although it is well known that theophylline is mainly metabolized to 1,3-DMU, 1-MX, and 3-MX by CYP1A2, we first found that CYP2A13 can metabolize theophylline. The clinical significance of CYP2A13 in the metabolism of phenacetin and theophylline in human liver would be limited because systemic clearance of drugs is caused by the metabolism in liver where

TABLE 3

Kinetic parameters for theophylline metabolism by recombinant CYP1As and CYP2As

Data are mean ± S.D. of three independent experiments.

	K_m	V_{max}	V_{max}/K_m
	mM	*pmol/min/pmol P450*	*nl/min/pmol P450*
8-Hydroxylation (1,3-DMU formation)			
CYP1A1	3.9 ± 0.1	5.1 ± 0.2	1.3 ± 0.1
CYP1A2	0.6 ± 0.0	24.4 ± 2.5	40.0 ± 4.0
CYP2A6	8.7 ± 0.4[a,b]	7.4 ± 0.3[a,b]	0.9 ± 0.0[a,b]
CYP2A13	2.5 ± 0.1[a,b]	10.3 ± 0.4[a,b]	4.1 ± 0.2[a,b]
3-Demethylation (1-MX formation)			
CYP1A1	11.1 ± 1.5	1.7 ± 0.2	0.2 ± 0.0
CYP1A2	0.6 ± 0.1	1.0 ± 0.2	1.8 ± 0.3
CYP2A6	N.D.	N.D.	N.D.
CYP2A13	1.4 ± 0.2[a,b]	0.2 ± 0.0[a,b]	0.2 ± 0.0[b]
1-Demethylation (3-MX formation)			
CYP1A1	N.D.	N.D.	N.D.
CYP1A2	0.6 ± 0.1	1.1 ± 0.2	1.8 ± 0.3
CYP2A6	N.D.	N.D.	N.D.
CYP2A13	N.D.	N.D.	N.D.

N.D., not detected.
[a] $P < 0.005$ compared with CYP1A1.
[b] $P < 0.005$ compared with CYP1A2.

CYP2A13 is hardly expressed. However, CYP2A13 is highly expressed in the respiratory tract. It has been shown that human lung is one of the tissues where local metabolism of xenobiotics may take place. Indeed, theophylline is distributed in the lung at the same concentration as in blood (Schack and Waxler, 1949); human lung microsomes can convert theophylline to 1,3-DMU (Bowen et al., 1991). Therefore, CYP2A13 possibly contributes to the theophylline metabolism in human lung and may cause a change in therapeutic efficacy, although other isoforms such as CYP1A1, CYP2E1, CYP2D6, and CYP3A4 expressing in human lung and having capability for theophylline metabolism (Zhang and Kaminsky, 1995; Bernauer et al., 2006) may also contribute to the extrahepatic metabolism.

We found that CYP2A13 shares substrates with CYP1A2. The amino acid homology between CYP2A13 and CYP1A2 is less than 40%. Even if we compared the amino acids within site recognition sites of CYP2A13 and CYP1A2, the amino acid homology is extremely low. In addition, three-dimensional quantitative structure-activity relationship analysis of CYP2A13 is not accomplished yet. Thus, although available information is limited, our data potentially suggested the structural similarity of the substrate binding site of CYP2A13 with that of CYP1A2. Recently, we found that CYP2A13 can catalyze the metabolic activation of 4-aminobiphenyl that is also known to be metabolized by CYP1A2 (Nakajima et al., 2006). Therefore, we investigated whether CYP2A13 is involved in the activation of other arylamines such as 2-aminofluorene, 2-amino-3,5-dimethylimidazo[4,5-*f*]quinoline, and 2-amino-1-methyl-6-phenylimidazo-[4,5-*b*]pyridine that were reported to be activated by CYP1A by umu assay. However, the metabolic activation of these compounds by CYP2A13 was not detected (data not shown). Thus, CYP2A13 may not necessarily be involved in the metabolism of substrates of human CYP1A.

In the present study, we found that CYP2A13 can metabolize several compounds that are known as the substrates of CYP1A2. CYP2A13 may play roles in the local metabolism of drugs in the human respiratory tract. This study significantly increased our understanding of the substrate specificity of human CYP2A13.

Acknowledgments. We thank Brent Bell for reviewing the manuscript.

Drug Metabolism and Toxicology, TATSUKI FUKAMI
Division of Pharmaceutical Sciences, MIKI NAKAJIMA
Graduate School of Medical Science, HARUKO SAKAI
Kanazawa University, MIKI KATOH
Kanazawa, Japan TSUYOSHI YOKOI

References

Bao Z, He XY, Ding X, Prabhu S, and Hong JY (2005) Metabolism of nicotine and cotinine by human cytochrome P450 2A13. *Drug Metab Dispos* **33**:258–261.
Bernauer U, Heinrich-Hirsch B, Tonnies M, Peter-Matthias W, and Gundert-Remy U (2006) Characterisation of the xenobiotic-metabolizing cytochrome P450 expression pattern in human lung tissue by immunochemical and activity determination. *Toxicol Lett* **164**:278–288.
Bowen J, Spino M, Tesoro A, Pop R, and Patterson A (1991) Theophylline (theo) biotransformation by human lung microsomes. *Clin Pharmacol Ther* **51**:178.
Bradford MM (1976) Rapid and sensitive method for the quantitation of microgram quantities of protein utilizing the principle of protein-dye binding. *Anal Biochem* **72**:248–254.
Eugster HP, Probst M, Wurgler FE, and Sengstag C (1993) Caffeine, estradiol, and progesterone interact with human CYP1A1 and CYP1A2. Evidence from cDNA-directed expression in *Saccharomyces cerevisiae*. *Drug Metab Dispos* **21**:43–49.
Fernandez-Salguero P, Hoffman SM, Cholerton S, Mohrenweiser H, Raunio H, Rautio A, Pelkonen O, Huang JD, Evans WE, Idle JR, et al. (1995) A genetic polymorphism in coumarin 7-hydroxylation: sequence of the human *CYP2A* genes and identification of variant *CYP2A6* alleles. *Am J Hum Genet* **57**:651–660.
Fukami T, Nakajima M, Yoshida R, Tsuchiya Y, Fujiki Y, Katoh M, McLeod HL, and Yokoi T (2004) A novel polymorphism of human *CYP2A6* gene *CYP2A6*17* has an amino acid substitution (V365M) that decreases enzymatic activity in vitro and in vivo. *Clin Pharmacol Ther* **76**:519–527.
Gallagher EP, Kunze KL, Stapleton PL, and Eaton DL (1996) The kinetics of aflatoxin B_1 oxidation by human cDNA-expressed and human liver microsomal cytochrome P450 1A2 and 3A4. *Toxicol Appl Pharmacol* **141**:595–606.
Gu J, Su Y, Chen QY, Zhang X, and Ding X (2000) Expression and biotransformation enzymes in human fetal olfactory mucosa: potential roles in developmental toxicity. *Toxicol Appl Pharmacol* **165**:158–162.
Hammons GJ, Milton D, Stepps K, Guengerich FP, Tukey RH, and Kadlubar FF (1997) Metabolism of carcinogenic heterocyclic and aromatic amines by recombinant human cytochrome P450 enzymes. *Carcinogenesis* **18**:851–854.
He XY, Shen J, Ding X, Lu AY, and Hong JY (2004) Identification of Val117 and Arg372 as critical amino acid residues for the activity difference between human CYP2A6 and CYP2A13 in coumarin 7-hydroxylation. *Arch Biochem Biophys* **427**:143–153.
He XY, Tang L, Wang SL, Cai QS, Wang JS, and Hong JY (2006) Efficient activation of aflatoxin B_1 by cytochrome P450 2A13, an enzyme predominantly expressed in human respiratory tract. *Int J Cancer* **118**:2665–2671.
Koskela S, Hakkola J, Hukkanen J, Pelkonen O, Sorri M, Saranen A, Anttila S, Fernandez-Salguero P, Gonzalez F, and Raunio H (1999) Expression of *CYP2A* genes in human liver and extrahepatic tissues. *Biochem Pharmacol* **57**:1407–1413.
Nakajima M, Itoh M, Sakai H, Fukami T, Katoh M, Yamazaki H, Kadlubar FF, Imaoka S, Funae Y, and Yokoi T (2006) CYP2A13 expressed in human bladder metabolically activates 4-aminobiphenyl. *Int J Cancer* **119**:2520–2526.
Nakajima M, Kobayashi K, Shimada N, Tokudome S, Yamamoto T, and Kuroiwa Y (1998) Involvement of CYP1A2 in mexiletine metabolism. *Br J Clin Pharmacol* **46**:55–62.
Nakajima M, Yamamoto T, Nunoya K, Yokoi T, Nagashima K, Inoue K, Funae Y, Shimada N, Kamataki T, and Kuroiwa Y (1996) Role of human cytochrome P4502A6 in *C*-oxidation of nicotine. *Drug Metab Dispos* **24**:1212–1217.
Ohyama K, Nakajima M, Suzuki M, Shimada N, Yamazaki H, and Yokoi T (2000) Inhibitory effects of aminodarone and its *N*-deethylated metabolite on human cytochrome P450 activities: prediction of in vivo drug interactions. *Br J Clin Pharmacol* **49**:244–253.
Omura T and Sato R (1964) The carbon monoxide-binding pigment of liver microsomes. *J Biol Chem* **239**:2370–2378.
Parikh A, Gillam EM, and Guengerich FP (1997) Drug metabolism by *Escherichia coli* expressing human cytochromes P450. *Nat Biotechnol* **15**:784–788.
Peng HM, Ding X, and Coon MJ (1993) Isolation and heterologous expression of cloned cDNAs for two rabbit nasal microsomal proteins, CYP2A10 and CYP2A11, that are related to nasal microsomal cytochrome P450 form a. *J Biol Chem* **268**:17253–17260.
Schack JA and Waxler SH (1949) An ultraviolet spectrophotomeric method for the determination of theophylline and theobromine in blood and tissues. *J Pharmacol Exp Ther* **97**:283–291.
Sesardic D, Boobis AR, Edwards RJ, and Davies DS (1988) A form of cytochrome P450 in man, orthologous to form d in the rat, catalyses the *O*-deethylation of phenacetin and is inducible by cigarette smoking. *Br J Clin Pharmacol* **26**:363–372.
Su T, Bao Z, Zhang QY, Smith TJ, Hong JY, and Ding X (2000) Human cytochrome P450 CYP2A13: predominant expression in the respiratory tract and its high efficiency metabolic activation of a tobacco-specific carcinogen, 4-(methylnitrosamino)-1-(3-pyridyl)-1-butanone. *Cancer Res* **60**:5074–5079.
Tassaneeyakul W, Birkett DJ, Veronese ME, McManus ME, Tukey RH, Quattrochi LC, Gelboin HV, and Miners JO (1993) Specificity of substrate and inhibitor probes for human cytochrome P450 1A1 and 1A2. *J Pharmacol Exp Ther* **265**:401–407.
Tiano HF, Hosokawa M, Chulada PC, Smith PB, Wang RL, Gonzalez FJ, Crespi CL, and Langenbach R (1993) Retroviral mediated expression of human cytochrome P450 2A6 in C3H/10T1/2 cells confers transformability by 4-(methylnitrosamino)-1-(3-pyridyl)-1-butanone (NNK). *Carcinogenesis* **14**:1421–1427.
Venkatakrishnan K, von Moltke LL, and Greenblatt DJ (1998) Human cytochromes P450 mediating phenacetin *O*-deethylation in vitro: validation of the high affinity component as an index of CYP1A2 activity. *J Pharm Sci* **87**:1502–1507.

von Weymarn LB and Murphy SE (2003) CYP2A13-catalysed coumarin metabolism: comparison with CYP2A5 and CYP2A6. *Xenobiotica* **33**:73–81.

Williams CH Jr and Kamin H (1962) Microsomal triphosphopyridine nucleotide-cytochrome c reductase of liver. *J Biol Chem* **237**:587–595.

Yamanaka H, Nakajima M, Fukami T, Sakai H, Nakamura A, Katoh M, Takamiya M, Aoki Y, and Yokoi T (2005) CYP2A6 and CYP2B6 are involved in nornicotine formation from nicotine in humans: interindividual differences in these contributions. *Drug Metab Dispos* **33**:1811–1818.

Yamano S, Tatsuno J, and Gonzalez FJ (1990) The CYP2A3 gene product catalyzes coumarin 7-hydroxylation in human liver microsomes. *Biochemistry* **29**:1322–1329.

Yamazaki H, Nakamura M, Komatsu T, Ohyama K, Hatanaka N, Asahi S, Shimada N, Guengerich FP, Shimada T, Nakajima M, et al. (2002) Roles of NADPH-P450 reductase and apo- and holo-cytochrome b_5 on xenobiotic oxidations catalyzed by 12 recombinant human cytochrome P450s expressed in membranes of *Escherichia coli*. *Protein Expr Purif* **24**:329–337.

Yasukochi Y and Masters BS (1976) Some properties of detergent-solubilized NADPH-cytochrome c (cytochrome P-450) reductase purified by biospecific affinities chromatography. *J Biol Chem* **251**:5337–5344.

Zhang ZY and Kaminsky LS (1995) Characterization of human cytochromes P450 involved in theophylline 8-hydroxylation. *Biochem Pharmacol* **50**:205–211.

Address correspondence to: Miki Nakajima, Drug Metabolism and Toxicology, Division of Pharmaceutical Sciences, Graduate School of Medical Science, Kanazawa University, Kakuma-machi, Kanazawa 920-1192, Japan. E-mail: nmiki@kenroku.kanazawa-u.ac.jp